



Numerical modelling of aeolian
coastal landform development

B. van Westen

Numerical modelling of aeolian coastal landform development

MSc Thesis

by

B. van Westen

to obtain the degree of Master of Science
at the Delft University of Technology,
to be defended publicly on Friday November 30, 2018 at 4:00 PM.

Student number:	4229010	
Thesis committee:	Prof. dr. ir. A. J. H. M. Reniers,	TU Delft
	Dr. ir. S. de Vries,	TU Delft
	Dr. ir. B. C. van Prooijen,	TU Delft
	Dr. ir. B. M. Hoonhout,	Van Oord
	Ir. J. P. den Bieman	Deltares
	Dr. M. E. B. van Puijenbroek,	Wageningen Marine Research
	Prof. dr. ir. P. Rauwoens	KU Leuven

An electronic version of this thesis is available at <http://repository.tudelft.nl/>.

Cover: Photograph obtained from <https://www.wereldwad.nl/ecotopen/duin/>

Preface

This thesis concludes the Master of Science program in Hydraulic Engineering at Delft University of Technology. The research has been carried out at the research institute Deltares. Their cooperation is hereby gratefully acknowledged.

I want to thank my entire graduation committee, Ad Reniers, Sierd de Vries, Bas Hoonhout, Joost den Bieman, Bram van Prooijen, Marinka van Puijenbroek and Pieter Rauwoens, for their interest, feedback and guidance. My sincere gratitude goes to Bas for giving me the opportunity to work on this topic and allowing me to continue the development of the AeoliS model. Also many thanks to Joost for taking over the role of supervisor from Bas halfway through the project. I would like to thank you both for all the support and making time whenever I needed advice. Sierd, many thanks for sharing your expertise, the many discussions and your enthusiasm towards the topic, which really reflected on my motivation. Thanks Ad for the advice during the project and always reminding me to keep the project feasible. I want to thank Marinka for her advice on ecology-related aspects and the provided measurement data. Also thanks to Bram for the interest in the project. Furthermore, I would like to thank Pieter Rauwoens with the help on the wind field implementation in the AeoliS model, Corjan Nolet for the provided measurement data and Bert van der Valk for the interesting information on dune development during the field trip to the Marker Wadden.

I also would like to thank my fellow graduate students for their interest, advice and of course all laughs during the coffee breaks. And last but not least, thanks to my friends and family. All the conversations on dunes and sand were probably not as interesting as I may thought, but your support and good times really kept me motivated throughout this thesis.

B. van Westen
Delft, November 2018

Abstract

Introduction

Coastal dunes serve as a first line of protection against flooding by the sea. In the recent past, the interest in secondary services provided by coastal dunes has increased. These services include ecological values and recreation. In order to manage and maintain the coastal as an attractive area that combines coastal protection, ecological values and recreation, the natural dynamics have to be understood. In view of this, numerical models with quantitative predictive capabilities on the development of coastal dunes provide a useful tool for coastal zone managers. However, many currently available models are more focused on the qualitative simulation of landforms. The aim is to improve the current aeolian modelling state of the art by implementing biological and physical processes adapted from different existing models, developing a modular aeolian transport model with quantitative predictive capabilities for dune development.

Several models for aeolian sediment transport and dune development are currently available. A general problem in modelling of aeolian transport is the over-prediction of actual transport rates on beaches, because models can only handle transport-limited situations (de Vries et al., 2014). This over-prediction limits the quantitative prediction of the development of coastal dune landforms. The AeoliS model (Hoonhout and de Vries, 2016a) is a process-based aeolian sediment transport model with spatiotemporal varying sediment availability, capable of simulating both supply- and transport-limited situations. However, AeoliS lacks dune building processes. Another model, the Coastal Dune Model (CDM) (Durán and Herrmann, 2006b; Durán and Moore, 2013; Sauermann et al., 2001), does contain dune building processes including a quantitative description of turbulent flow fields over smooth hills, a continuum saltation model and avalanching. In cases where beach dune vegetation dynamics are significant, Dune-Beach-Vegetation (DUBEVEG) (de Groot et al., 2012) provides a practical implementation of vegetation dynamics.

Method

We have combined model formulations of three aeolian transport and dune models Aeolis, CDM and DUBEVEG in a single model. The supply-limited approach from AeoliS is combined with the dune development processes and general formulas for vegetation growth and their influence on the shear stresses from CDM. Vegetation parameters as germination and lateral expansion are adapted from DUBEVEG. In order to reproduce the influence of the sea, marine sediment supply in the intertidal zone and the mechanical erosion of sediment and vegetation during extreme events are implemented as well.

Results

The combined model is now capable of simulating barchan dunes. The general dimensions and migration velocities are in the same order of magnitude as in earlier CDM simulations. As a result of several numerical issues the simulation of parabolic dunes is not yet capable. The inclusion of seed germination and lateral vegetation expansion causes the growth of randomly located hummocks, creating embryo dune fields. The shape of single embryo dunes and development of embryo dune fields is reproduced reasonably well by the model.

Conclusion and Outlook

We have assembled a modular model for prediction aeolian sediment transport and dune development for coastal situations. The modular structure of the model makes it possible to couple it to hydrodynamic-, groundwater- or vegetation-models, with the eventual possibility to simulate complete coastal areas. The model can be used to determine the influence of tidal ranges, storm frequencies, armoring, salinity and precipitation on dune building processes. This will result in a greater insight in the general behavior of coastal systems, including the evolution of embryonal dune fields as well as foredune characteristics like maximum height and autocyclic formation of transversal dunes. On the other hand the model can also be used during more practical situations such as computing recovery times of coastal dunes after extreme events or for the creation of artificial blowouts.

Contents

List of Symbols	ix
1 Introduction	1
1.1 Relevance of predicting coastal landform development	1
1.1.1 Climate change	1
1.1.2 Dynamic preservation of the Dutch coastline	2
1.2 Dune development	4
1.3 Landforms	5
1.3.1 Desert Dunes	5
1.3.2 Coastal dunes	6
1.4 Numerical modelling	8
1.5 Objectives	9
1.6 Reader	9
2 Literature on coastal landforms	11
2.1 Processes governing coastal landform development	11
2.1.1 Aeolian sediment transport	11
2.1.2 Wind Fields	12
2.1.3 Avalanching	14
2.1.4 Non-erodible elements	14
2.1.5 Vegetation	14
2.1.6 Marine processes	18
2.2 Landforms	20
2.2.1 Barchan dunes	20
2.2.2 Parabolic dunes	20
2.2.3 Embryo dunes	21
2.2.4 Foredunes	23
2.3 Numerical models related to coastal landforms	24
2.3.1 Coastal Dune Model	24
2.3.2 DUBEVEG	25
2.3.3 AeLiS	25
2.3.4 Overview of processes and models	26
3 Method	27
3.1 Implementation of processes	27
3.1.1 Aeolian sediment transport	27
3.1.2 Wind field	29
3.1.3 Avalanching	30
3.1.4 Non-erodible layer	31
3.1.5 Vegetation	31
3.1.6 Swash zone interaction	32
3.2 Landform simulation	33
3.2.1 Barchan dunes	33
3.2.2 Parabolic dunes	33
3.2.3 Embryo dunes	35
4 Results	37
4.1 Processes	37
4.1.1 Wind fields	37
4.1.2 Aeolian transport	39
4.1.3 Avalanching	39

4.2	Simulation of landforms	40
4.2.1	Barchan dunes	40
4.2.2	Parabolic dunes	43
4.2.3	Embryo dunes	44
5	Discussion	49
5.1	Model limitations	49
5.1.1	Aeolian sediment transport	49
5.1.2	Wind fields	50
5.1.3	Avalanching	50
5.1.4	Vegetation	51
5.1.5	Hydrodynamics	52
5.2	Simulation of landforms	52
6	Conclusion	53
7	Recommendations	55
7.1	Advection equation	55
7.2	Sediment transport	55
7.3	Vegetation, meteorology and groundwater	56
7.4	Flow separation	56
7.5	Coupling with hydrodynamic models	56
A	Conceptual scheme of model	57
B	Advection Scheme	59
B.1	Advection scheme comparison	59
B.2	Advection scheme in new model	60
C	Redefined Grid Parameters	63
	Bibliography	65

List of Symbols

α	Constant in transport equation	-
γ	Constant accounting for splash process in saltation model	-
Γ	Roughness factor of vegetation on shear stress	-
γ_{veg}	Constant representing importance of sediment burial to vegetation growth	-
γ_w	Maximum wave height over depth ratio	-
$\Delta z_{b,opt}$	Shift of the peak for optimum vegetation growth	m/year
θ	Fixation index related to parabolic dune development	-
θ_c	Critical value for fixation of parabolic dunes	-
θ_{dyn}	Dynamic angle of repose	deg
θ_{stat}	Static angle of repose	deg
κ	Von Kármán parameter	-
ξ	Surf similitrity parameter	-
ρ_a	Air density	kg/m ³
ρ_s	Sediment density	kg/m ³
ρ_{veg}	Vegetation cover	-
τ	Shear stress	N/m ²
τ_{th}	Shear stress threshold	N/m ²
τ_s	Effective shear stress on grains	N/m ²
c	Actual sediment concentration	kg/m ²
c_{sat}	Saturated sediment concentration	kg/m ²
d	Grain diameter	m
g	Gravitational acceleration	m/s ²
H_s	Significant wave height	m
h_{veg}	Vegetation height	m
H_{veg}	Maximum vegetation height	m
n	Porosity	-
$p_{establish}$	Probabilistic value for establishment of vegetation	m ² /year
$p_{lateral}$	Probabilistic value for the lateral propagation of vegetation	m ² /year
Q	Sediment transport	kg/m/s
Q_0	Sediment transport over a flat bed	kg/m/s
R	Wave run-up	m
T	Adaptation time scale	s
T_{dvl}	Duration time scale for hydrodynamics influencing vegetation	s
T_{swash}	Duration time scale for hydrodynamics influencing the morphology	s
u_*	Shear velocity	m/s
u_{*th}	Shear velocity threshold	m/s
u_s	Grain velocity	m/s
u_z	Wind velocity at height z	m/s
ν	Kinematic viscosity	m ² /s
V_{veg}	Characteristic vegetation growth	m
z_0	Bed roughness	m
z_1	A height within the saltation layer	m
z_b	Bed level	m
z_m	Height of the saltation layer	m
z_s	Water level	m
z_{sep}	Height of separation bubble	m

Introduction

Coastal landforms develop under the influence of interaction between aeolian, biological and hydrodynamic processes. Coastal dunes can serve as a first line of coastal defense that protects the hinterland from flooding by the sea. Besides, coastal areas provide biodiverse ecosystems, popular recreational services and store drinking water. However, conditions are changing and the interest in coastal dune development is shifting.

Numerical modelling of aeolian coastal processes can serve as a tool for engineering purposes, increasing the quantitative predictability of coastal dune development. In this introduction, the main changes in conditions, causes of shifted interests, the processes governing coastal landform development and the necessity and current state of numerical modelling will be discussed.

1.1. Relevance of predicting coastal landform development

Coastal dunes serve as a first line of protection against the sea worldwide. Around 34% of world's the ice-free coasts are occupied by coastal dunes (Hardisty, 1994). However, uncertainties concerning coastal dune development are increasing due to climate change and shifting dune management strategies.

1.1.1. Climate change

Due to the climate-change-induced sea level rise, the preservation and development of coastal dunes is in danger. The expected sea level rise will negatively affect the sediment budgets of the coastal systems, resulting in retreat of the shoreline and eventually the erosion of dunes (Ranasinghe et al., 2012). The general expected response of coastal dunes to sea level rise is shown in figure 1.1, however a lot of research is required to be able to estimate the exact consequences (Keijsers, 2015).

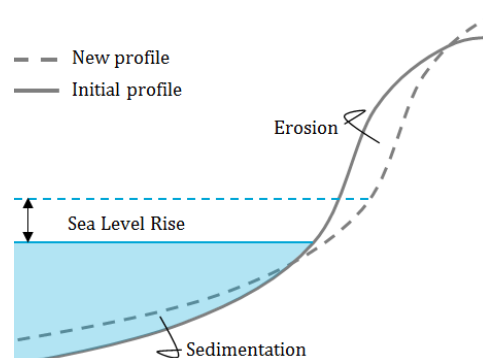


Figure 1.1: The response of a coastal dune profile to sea level rise.

On top of sea level rise, also changes in wind and wave climate (van den Hurk et al., 2007) affect the development of coastal dunes. It is expected that the frequency and strength of storms will increase, resulting in more foredune erosion under wave attack. During calm conditions, coastal dunes recover towards an equilibrium profile, partly due to the aeolian transport of sediment from the beach to the dunes, which is shown in figure 1.2. Since the influence of extreme weather events is expected to increase, it is important to be able to estimate the time required for full coastal dune recovery. For instance, in case that the safety of an area prone to hurricanes must be assessed, not only the damage after a single hurricane is necessary, but also the time required to recover the damaged dune before the next hurricane arrives.

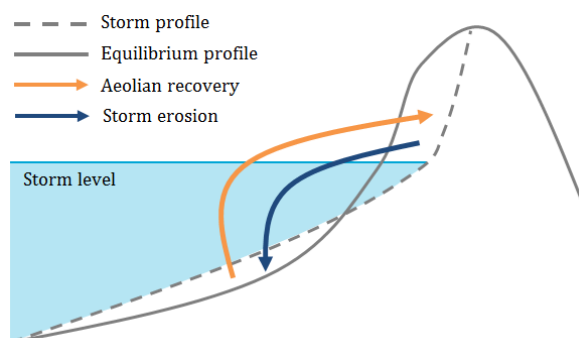


Figure 1.2: Schematisation of storm and equilibrium profiles due to hydrodynamic erosion and aeolian recovery.

Besides external conditions, such as climate change, also shifts in coastal management strategies influence the development of coastal dunes. The reason and consequences of a new management approach adopted in the recent past will be discussed.

1.1.2. Dynamic preservation of the Dutch coastline

Large stabilized coastal landforms can be found along the Dutch coastline. It is estimated that these landforms were already stabilized in the 16th century as a result of human intervention, in order to protect villages from the migrating dunes (Bakker et al., 1981).

Since the construction of the *Afsluitdijk* (1932) the Dutch coastline is dealing with severe erosion. As a result, the shoreline started to retreat and the existence of coastal dunes was threatened. The planting of marram grass was required to strengthen the foredune and guarantee the safety of the hinterland against the sea.

Due to the complete stabilization of the coastal area, the characteristic ecosystem started to disappear. A continuous ridge was created separating the coastal zone from the hinterland. Coastal vegetation requires the refreshment of calcareous sediment from the beach, reducing acidification of the soil, driving growth of new vegetation. Besides, the typical dune vegetation became overgrown by the planted vegetation and the groundwater table declined. The combined consequences of human interventions changed the coastal landscape from a biodiverse, unique and dynamic system to a static forest-like area. On top of the reduced ecological and recreational values, it is often believed a more dynamic system is better capable of adjusting to the changing conditions, such as climate change induced sea level rise.

In 1990, a new maintenance policy was implemented in the Dutch national law; maintaining the entire coastline at its 1990 position, which meant the placement of sand nourishments in order to counteract the further expected erosion (Rijkswaterstaat, 1990). This new strategy was called *dynamic preservation of the coastline* and as a result, the coastal situation changed and new engineering approaches emerged.

Emergence and creation of blowouts

As a consequence of the new coastal management strategy, foredune volume started to grow instead of the previous observed decay. At several locations, the planting of marram grass was no longer necessary, allowing the return of a dynamic character in the coastal area. The ending of the foredune maintenance stimulates the emergence of blow-outs: Areas with limited protection by vegetation causing a local increase of sediment transport. An example of a growing blowout is shown in figure 1.3. These recent developments stimulate the return of a dynamic character of coastal dunes (Arens and Mannaart, 2008; Arens, 2017; Loffler et al., 2016).

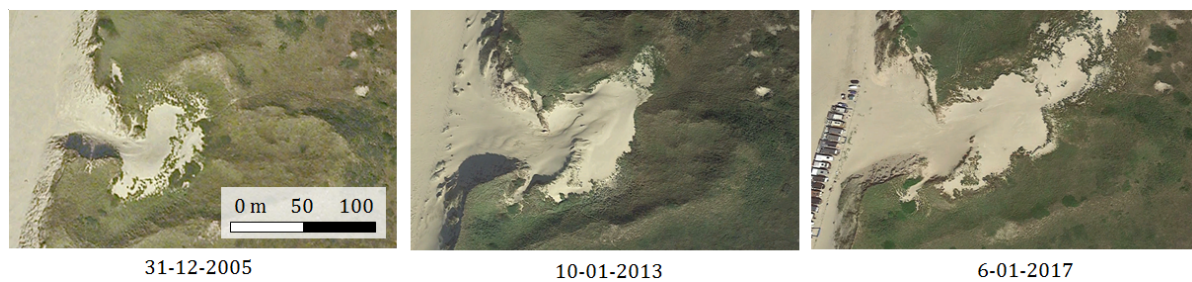


Figure 1.3: Blowout development in coastal dunes near Castricum (Noordhollands Duinreservaat). Retrieved from [Google Earth](#).

In the recent past, blowout formation is artificially stimulated by directly excavating parts of dunes and the removal of vegetation and trees. ([Ministerie van Economische Zaken and Ministerie van Infrastructuur en Milieu, 2017](#); [PWN, 2018](#)). An example of such a project is the reintroduction of natural dynamics in the Schoorlse Duinen, where forests are removed and parts of dunes are excavated ([Staatsbosbeheer](#)) to allow the remobilization of the area.

Although ecological values are increased, not much is known about the consequences of such measures on the protective function of the coastal foredune. Dynamic coastal management is only allowed at locations where the coastal safety is guaranteed. Besides, the combination with other purposes, such as recreation and drinking water facilities could cause problems ([Rijkswaterstaat and STOWA](#)). In order to expand the range of potential locations for dynamic coastal management, the quantitative predictability of such a dynamic system should be improved.

Another consequence of the dynamic coastal management is a mobilization of dunes. Since the stabilization of the coastal dunes was initially intended to protect villages from the migrating dunes, the remobilization of the area could reintroduce these problems. The moment of mobilization, migration velocity and volumes are not known and therefore it is not possible to estimate the consequences of remobilization.

The Sand Motor

Another new coastal maintenance strategy is the placement of mega-nourishments. Following the Building with Nature philosophy ([Ecoshape; van Slobbe et al., 2013](#)), it uses the power of wind, waves and tide to spread sediment along the adjacent coast. To aim is to achieve a more sustainable nourishment approach, mitigating the negative effects of multiple smaller sand nourishments.

In 2011, a mega-nourishment is built along the Dutch coastline: The Sand Engine, also known as the Sand Motor ([Stive et al., 2013](#)). The nourishment had a total volume of 21 M m^3 and is designed to protect the Delfland coast for approximately 20 years. The mega-nourishment will eventually result in wider beaches at the adjacent coastlines and more volume in the coastal dune areas. This way, defense against flooding, drink water storage, recreational area and other services that coastal dunes provide us, are preserved.

The Sand Motor is a relatively high elevated and wide area, so dune development conditions differ from natural beaches. Due to the high elevation the growth of vegetation is not negatively affected by storms, soil salinity or salt spray. However, the ground water table is relatively low and the marine dispersion of seeds is restricted. Due to the age of the nourishment, it can be expected that nutrients are lacking and the recreational nature of the area causes unknown anthropogenic influences.

These altered conditions result in uncertainty concerning dune development in the Sand Motor domain. [Hoonhout and de Vries \(2017\)](#) found that the dune growth in the Sand Motor domain is low compared to adjacent coasts. This could be explained by the presence of the lagoon blocking the supply of sediment, but could also be an effect of beach armouring. An armour layer blocks aeolian sediment transport, because it consists of coarser sediment particles. Due to the Sand Motors high elevation, the armour layer never gets mobilized like on "normal" beaches. Since dune development directly depends on sediment supply, it could be a partial explanation of the limited dune growth.

Increase predictability of coastal dune development

In order to create a coastal area that is ready to withstand climate change and allow dynamic coastal management, the quantitative predictability of coastal areas must be increased:

- Due to the expected sea level rise, the existence coastal (fore)dunes is threatened. It is uncertain how the coastal system will react to the climate change induced sea level rise.
- The required time for the aeolian recovery of coastal dunes after extreme weather events becomes more important, since it is expected that the frequency and strength of storms are increasing.
- In order to increase the amount of potential locations for dynamic coastal management, the predictability of the consequences on coastal safety and dune migration must be increased.
- To improve the design for future mega-nourishments, the effect of beach armouring and limited seed dispersion due to the high elevation of the bed on the Sand Motor must be better understood.

These are only several examples of situations which require increased predictability. Numerous other projects that are currently initiated or already running could benefit from better predictability. Examples of other projects following the Building with Nature philosophy are the Hondsbossche Dunes and the Marker Wadden ([Ecoshape](#)). Recent research has been performed on the influence of beach buildings on dune development ([Hoorhout and Waagmeester, 2014](#)). General knowledge on the development of coastal landforms is missing, such as the processes causing the maximum height of foredunes and the characteristics of auto-cyclical behaviour of foredunes ([Durán and Moore, 2013](#); [Moore et al., 2016](#)).

In order to get a better overview on the processes influencing the dune development, a short introduction on the governing dune development processes will be given.

1.2. Dune development

Dunes are a result of the interaction between physical and biological processes. An overview of these processes is shown in figure 1.4. The main process driving dune development is the sediment transported by wind: Aeolian sediment transport. The movement of particles at a sandy bed is caused by shear stresses exerted on the particles by the wind.

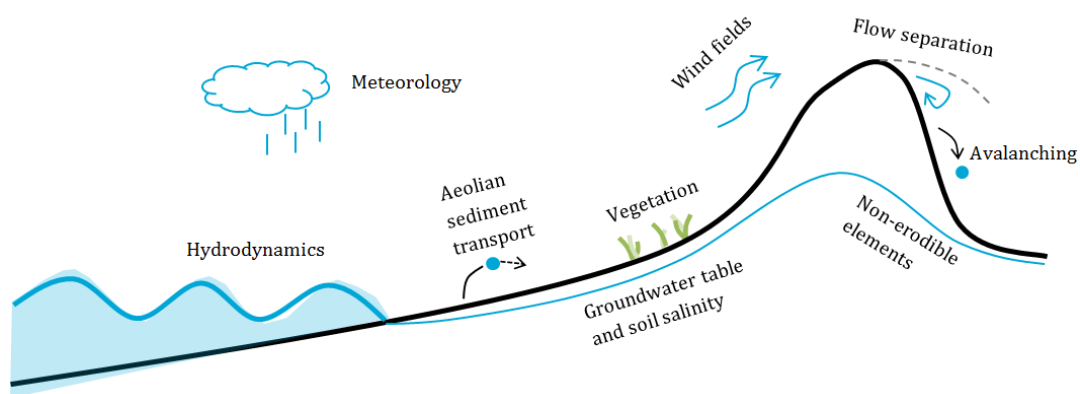


Figure 1.4: Schematic representation of the relevant processes related to coastal dune development

The aeolian transportation of sediment is classified into different modes. The finest sand particles are transported through suspension. The particles are lifted into the air and can be transported over long distances. An increase in grain size results in a greater influence by gravity and therefore larger particles make successive jumps rather than long distance transportation through the air, which is called saltation ([Bagnold \(1936\)](#)). After impact with the surface, the transported particle can bounce back or eject other particles into the air. The transportation of particles after impact of another particle is called reptation. When the particles are too large to be lifted, they can be transported by rolling and sliding along the bed surface, which is called creep. A schematisation of the different modes of aeolian transport is shown in figure 1.5.

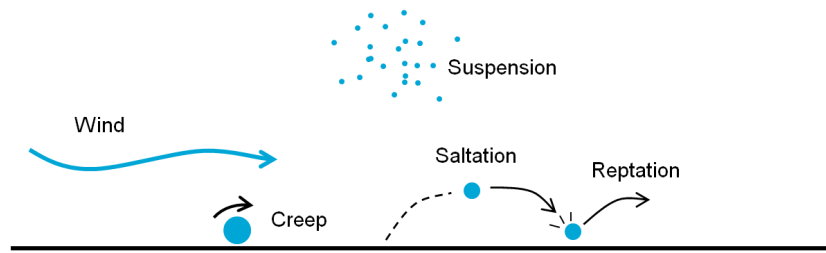


Figure 1.5: Different modes of aeolian transport

Interaction between wind fields and the topography create small perturbations in the wind field, which means that the wind speed spatially varies. Since wind velocities directly affects sediment transport, spatial variation in the wind field causes gradients in sediment transport. These gradients result in a pattern of erosion and sedimentation, initiating dune development. In order to initiate this process, some disturbance has to be present on the beach, which could be some piece of driftwood, garbage or vegetation.

The presence of vegetation causes the wind to slow down and therefore enhance the deposition of sand. Therefore vegetation can have a stabilizing effect on dunes. The establishment of vegetation starts with the dispersion and germination of a seed or rhizome. The growth of vegetation can be divided into the local change in biomass and the lateral propagation. Depending on the species, growth is influenced by numerous conditions, such as temperature, groundwater table, salinity, sediment burial and anthropomorphic influences. Vegetation can be destroyed during extreme events due wave impact.

Onces slopes become too steep, avalanches occur. This could be the result of erosion by hydrodynamic processes during extreme events on the seaward side or as a result of slopes formed by interaction between vegetation and aeolian processes.

The presence of a non-erodible layer can limit the sediment transport. Examples of these are layers of clay or human structures such as concrete slabs or beach houses. The groundwater table also acts as an non-erodible layer, due to the increase surface moisture content.

The presence of a shoreline affects dune development by the erosion of vegetation and dunes during extreme events and the influence on vegetation growth by the varying groundwater table and increased soil salinity concentrations. The presence of the shoreline can enhance sediment transport, because the waves mix up the top layer, preventing the process of armouring, but can also limit sediment transport because of an increase surface moisture content.

Meteorological processes such as sunshine and precipitation have an influence on sediment transport and vegetation growth.

1.3. Landforms

The interaction between all the mentioned processes result in numerous different types of dunes, varying in shape, size and mobility. The difference between dunes in desert and coastal areas is that desert dune development is not influenced by the presence of vegetation or a shoreline. Therefore the desert dunes formation is a result of mainly aeolian processes. The distinction between desert and coastal dunes will be used to get a better insight in the individual influence of the different processes on landform development.

1.3.1. Desert Dunes

Various types of desert dunes appear all over the world, which can be categorized by their shape. In an ideal situation with unimodal winds and a limited amount of available sediment, barchan dunes will develop. Barchan dunes are crescent-shaped, isolated dunes that are highly immobile. The upwind part of the dune, the windward side, is separated by the brink line from the slip face. At both sides of a barchan dunes, horns are formed, see figure 1.6.

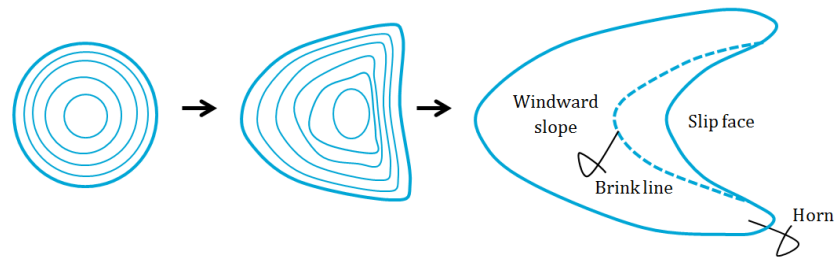


Figure 1.6: Top view of barchan dune development

An increase in sediment availability will result in the development of more barchan dunes and eventually these will start to compound. If the sediment availability is abundant, transverse dunes will start to develop. Transverse dunes are large, elongated dunes with a gentle slope at the windward side and a steep downwind of the crest.

A more diverse wind direction causes other desert dune shape variation. In a situation with moderate direction variation linear dunes are developed and for a even more complex wind regime reversing or star dunes will arise. An overview of the different desert dunes is given in figure 1.7.

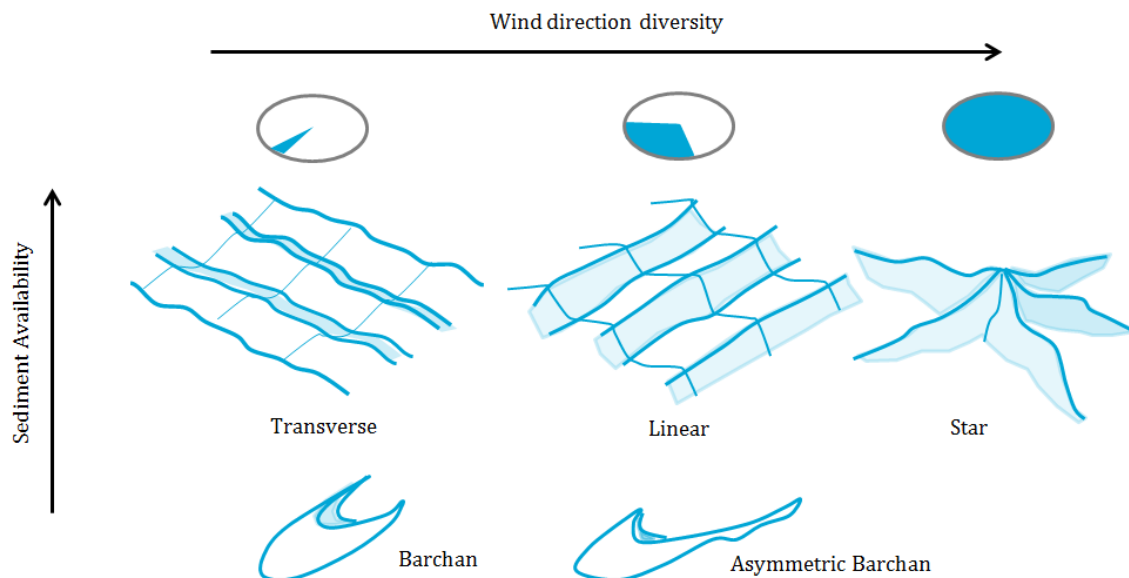


Figure 1.7: Overview of several shapes for desert dunes, modified from Parsons and Abrahams (2009)

1.3.2. Coastal dunes

Where desert dunes are highly mobile, coastal dunes can be stabilized by vegetation. The way stabilization by vegetation works can be best explained by the development of a parabolic dune from a barchan dune (Durán and Herrmann, 2006a).

Vegetation is not likely to grow in areas that have an erosive trend or where too much sedimentation occurs. Due to the varying flow velocities over a barchan dune, the sedimentation is spatially varying. The windward side of a barchan dune encounters an erosive trend so consequently vegetation is not likely to grow on that side of the dune. At the slipface of the dune, a lot of sedimentation occurs, so vegetation is also limited on that area. The magnitudes of sedimentation around the horns are relatively small, so these are getting occupied by vegetation. The grown vegetation reduces the wind velocity, captures sediment and stabilizes the horns, see figure 1.8.

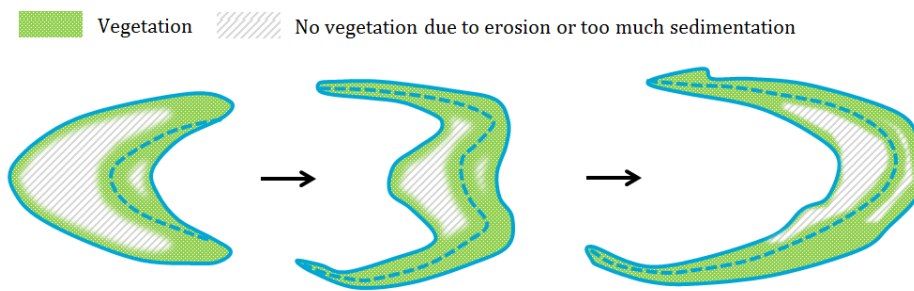


Figure 1.8: Transformation from a barchan dune to a parabolic dune due to vegetation

The description of the development of a parabolic dune out of a barchan dune is an academic case, which will not be observed in reality. However, parabolic dunes do occur along the Dutch coast as a result of blowouts. The emergence of a blowout is generally the same process as the parabolic dune development described above. Therefore, the shape of the coastal dunes depends on the vegetation density, see figure 1.9.

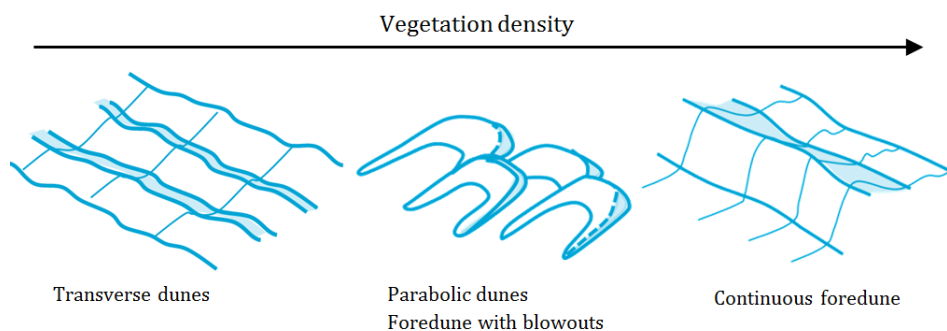


Figure 1.9: An overview of different coastal dune types due to varying species

Another difference between desert and coastal dunes development is the influence from the marine zone. Hydrodynamic processes cause erosion and accretion in the intertidal zone and increase the velocity threshold due to an increased surface moisture content. Besides, during storms vegetation can be destroyed and high salinity rates limit the growth of vegetation.

Embryo dunes are the initial phase of coastal dune formation. The main dune building species in western Europa are *Elytrigia juncea* (sand couch) and *Ammophila arenaria* (marram grass). It is generally assumed that the formation of embryo dunes starts by the establishment of sand couch, a pioneer, see figure 1.10. Once vegetation has established, the surface shear stress will be reduced, sediment will start to deposit and the heap of sand starts growing. If the embryo dune is large enough, rainfall can collect inside and a freshwater lens can develop. This creates the possibility for the dune-building species to establish.



Figure 1.10: *Ammophila arenaria* (left) and *Elytrigia juncea* (right) (Retrieved from <https://www.ecomare.nl/>)

Storms can cause the mechanical erosion of the vegetation and embryo dunes. Depending on the frequency, interval and severeness of storms, embryo dune development is limited by these extreme events. Marram grass is less salinity tolerant, but can better withstand the high stresses during extreme events due to a higher vegetation density. Over time, marram grass will out compete sand couch, which results in steeper and higher dunes and eventually the embryo dunes will grow into foredunes.

1.4. Numerical modelling

Models are simplifications of reality that can be useful to help to better understand complex phenomena and can therefore be used as tools for solving engineering problems. Numerical models are mathematical models that describe some phenomena, solving equations while often looping through time-steps and a spatial grid. Numerical models that simulate by representation of physical processes are called process-based models.

Over the last 20 years a lot of research has been carried out to improve the predictive skills of numerical models, but models are still subject to a considerable amount of uncertainty. Nevertheless these types of models can be very useful, also for filling the knowledge gap described in section 1.1.2.

Currently, several numerical models are available related to aeolian processes and/or coastal dune development. *AeoLiS* (Hoonhout and de Vries, 2016a) is a process-based model developed for the simulation of aeolian sediment transport in supply-limited situations, such as coastal areas. Examples of supply-limited situations are surface moisture and beach armouring. However, the interaction between wind fields and morphology is not implemented, so the model is not capable of describing dune development.

Coastal Dune Model (*CDM*) (Durán and Herrmann, 2006b; Durán and Moore, 2013; Kroy et al., 2002; Sauermann et al., 2001) is a model that is capable of describing dune development, but quantitative predictability is limited since several processes are described by empirical formulations, such as sediment availability and vegetation zoning.

DUNE BEACH VEGETATION (*DUBEVEG*) (Baas, 2002; de Groot et al., 2011; Keijsers, 2015; van Oene et al., 1999) is a cellular automaton with a probabilistic approach on the formation of dune and vegetation growth. The *DUBEVEG* approach is computationally fast, but limits the quantitative predictive skills of the model.

To fill up the knowledge gap, a process-based model with quantitative description of aeolian processes and dune development suitable for engineering purposes is required. None of the individual models fully satisfies these requirements, however a combination of these model capabilities could provide the solution.

1.5. Objectives

During this project the capabilities of different numerical models and the addition of several processes must result in a new model which is capable of quantitatively predicting coastal dune development and is suitable as a tool for engineering purposes. In order to evaluate the capabilities of the model, simulations of several landforms will be evaluated: Barchan, parabolic and embryo dunes (figure 1.11).

The main **objective** during this thesis is:

Develop a numerical model that is capable of quantitatively predicting realistic aeolian landforms and evaluate the simulation with the model of typical landforms.

This objective will be fulfilled by answering the following **research questions**:

I. Is the model capable of simulating the development of:

- A. Barchan dunes?
- B. Parabolic dunes?
- C. Embryo dunes?



Figure 1.11: Overview of the validation landforms during the thesis.

II. How is the development of landforms influenced by the implementation of processes related to:

- a. Aeolian sediment transport?
- b. Wind field?
- c. Avalanching?
- d. Non-erodible elements?
- e. Vegetation?
- f. Hydrodynamics?

1.6. Reader

This report starts with a literature review in chapter 2. The processes behind dune development will be discussed and if relevant, a short description on the implementation of the process in the various numerical models will be given (section 2.1). Subsequently, the available literature and measurements on landforms development will be discussed (section 2.2). Afterwards, an overview of the current state of the art of the available numerical models related to dune development and/or aeolian transport (section 2.3).

In chapter 3 the method of development of the model and the model configuration for the landform simulation will be discussed. First the technical background of the implementation will be described, including an elaboration on made decisions (3.1). The model configuration for the different landform simulations will be given in section 3.2.

An overview of the simulation results will be given in chapter 4, showing the influence of the individual processes in section 4.1 and the landform simulation results in section 4.2. Chapters 5, 6 and 7 are the discussion, conclusion and recommendations respectively.

2

Literature on coastal landforms

In this chapter an overview will be given of the current state of coastal dune modelling. The different processes influencing dune development will be discussed, including the various methods describing these processes. Afterwards, the formation and development of the mentioned landforms and measurements that are carried out on these landforms will be elaborated. Finally, the current state of the numerical models related to coastal dune development will be described and the implementation approach of the processes for each model will be discussed.

2.1. Processes governing coastal landform development

2.1.1. Aeolian sediment transport

The first saltation model that described aeolian transport was developed by [Bagnold \(1937\)](#). Once the wind near the bed reaches a certain velocity, the velocity threshold, motion is initiated and consequently sand particles get transported. In this formulation the aeolian transport rate is defined as a function of the shear velocity to the third power. The shear velocity is the only parameter limiting the sediment transport and therefore this type of formula is called **transport-limited**. A transport-limited situation is schematized in figure 2.1 (a).

Transport-limited formulations are valid for situations with wide open areas with sufficient sediment availability, such as desert areas. This differs from the situations in coastal areas, since the shoreline increases the surface moisture content, limiting sediment transport. In onshore direction, sediment transport increases it reaches the maximum capacity ruled by the wind velocity. The length of the sandy area over which the wind can pick up the sand particles is called the fetch area. [Bauer and Davidson-Arnott \(2003\)](#) proposed a model which included the effect of **fetch-limited** sediment transport, in which transport-limited formulation defined the maximum transport rate. The fetch-limited approach is shown in figure 2.1 (b).

The fetch-limited approach is an analytical representation of the time-averaged tidal influence. A more process-based representation of the shoreline influence is a time varying velocity threshold related on the water level elevation. Such an approach is called **supply-limited** transport ([de Vries et al., 2014](#)). Since supply-limited transport describes limitations to sediment transport on a process-based approach, other spatiotemporal limitations to sediment transport can also be described. Examples of these processes the effect of meteorology on surface moisture content, the emergence of non-erodible roughness elements and the sheltering of fine grains behind coarser ones (beach armoring). The influence of a sediment availability limited situation and the influence of tide are shown in figure 2.1 (c).

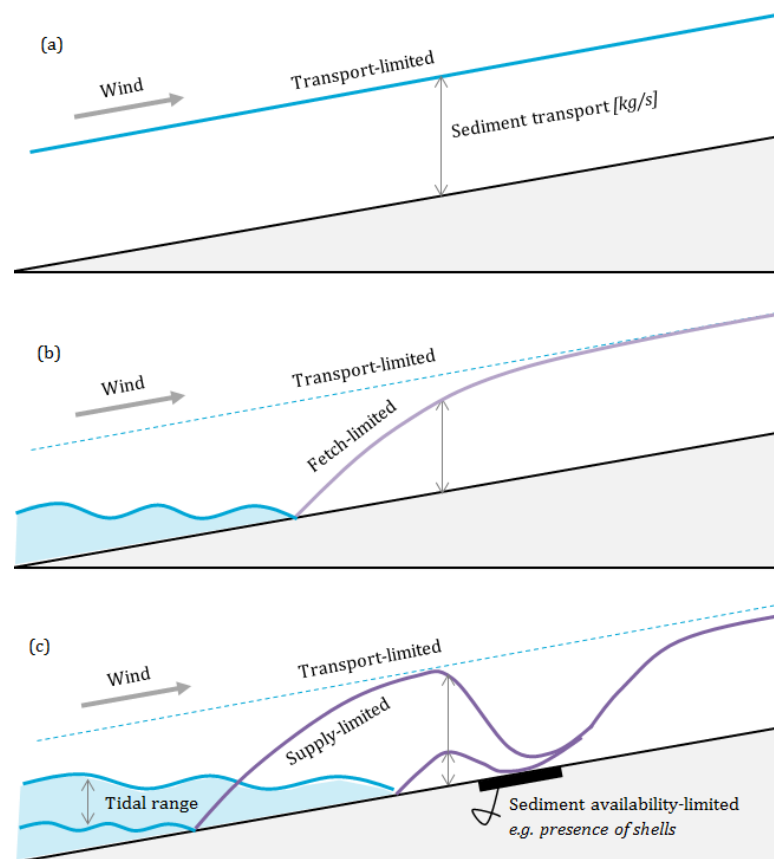


Figure 2.1: Schematisation of a transport-limited (a), fetch-limited (b) and supply-limited (c) approach.

2.1.2. Wind Fields

The interaction between morphology and wind fields causes spatial variations in shear stresses. These spatial variations result in varying sediment transports and eventually erosion and deposition patterns. The spatial variation of wind fields enables the development of dunes.

In order to describe the interaction between morphology and wind fields, a one dimensional hill will be used as an example, see figure 2.2. When streamlines encounter a smooth hill, divergence of the streamlines occur at the toe and starts to converge towards the top of the hill. At the lee side, the streamlines diverge again. The convergence of streamlines leads to acceleration of the wind and therefore in an increased shear stress, while divergence leads to deceleration and a decreased shear stress.

In a domain with a uniform shear stress, the amount of sediment coming into the domain is equal to the amount that is going out. In a situation with accelerating winds, as for the uphill slope, the sediment influx is lower than the sediment out flux, which results in an erosive trend. At the downhill slope, the opposite process occurs. So in the used example, erosion of sediment occurs at the uphill slope, which is deposited downhill. This results in the migration of the hill in windward direction.

The wind flow over a dune consists of a laminar part, which is symmetric, and a turbulent, asymmetric part (Kroy et al., 2002). While the contribution of the laminar part is dominant, the small turbulent part causes a phase lag between the dune profile and the shear stress profile. The peak of the shear stress profile is slightly upwind of the crest. Due to this phase lag the height of the dune can be affected, since deposition of the sediment starts in front of the crest, see figure 2.2.

The growth of the dune is restricted by another mechanism. When the shear velocity changes, the sediment flux requires a certain length in order to adjust to the new equilibrium. Therefore, there is a spatial lag between the shear stress and the sediment transport. The length over which the sediment flux relaxes in order to reach the fully saturated equilibrium state is the saturation length Sauermann et al. (2001).

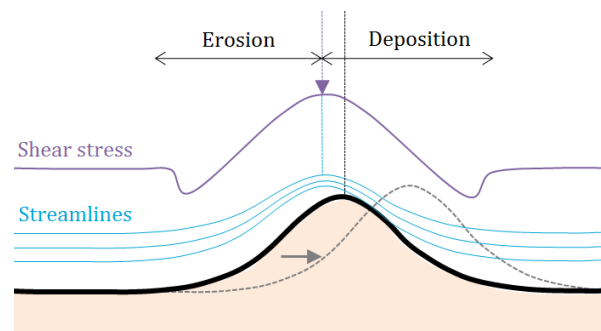


Figure 2.2: Schematisation of dune migration and formation due to modified wind fields

To be able to model a wind field over a sand dune, a better understanding of the turbulent flow field should be gained. However, solving turbulence is computationally expensive for a dune development model. [Weng et al. \(1991\)](#) proposed an analytical perturbation theory for turbulent boundary layer flow over smooth hills. Since this is an analytical solution, it is suitable for a large-scale dune development model, without the need of relatively heavy computations.

The theory of turbulent flow over smooth hills is only valid for smooth surfaces. At the top of dunes, sharp edges and steep slopes can be present. The described analytical model does not include nonlinear effects like the separation of the flow. In order to make the flow model suitable for dune formation, [Sauermann et al. \(2001\)](#) suggested the implementation of a separation bubble, which is defined as the surface that limits the region of recirculating flow behind the brink resulting from the separation of flow. Within the separation bubble, [Kroy et al. \(2002\)](#) stated that the flow velocity is low compared to the velocity threshold (see figure 2.3 (a)), thus it is acceptable that the flow velocity is assumed to be zero, see section 2.3.

[Parteli et al. \(2014b\)](#) discussed two missing secondary flow effects in the separation bubble. The assumption that the velocity is low compared to the velocity threshold is valid for a time-averaged situation, but due to turbulence it could happen that the threshold is exceeded during peaks. Therefore an improvement to the separation bubble would be the addition of reversed flow, see 2.3 (c). The other secondary effect [Parteli et al. \(2014b\)](#) discussed is the spiral flow along the crest of a dune as a result of oblique incoming winds, see figure 2.3 (b).

In the situation of more rugged shapes, like buildings, fences or rocks, flow separation occurs in a three dimensional space, see figure 2.3 (d). The separation bubble by [Sauermann et al. \(2001\)](#) only describes the vertical separation at the lee side of a dune. If one wants to model for instance the influence of beach houses on dune development, this three dimensional flow separation should be taken into consideration.

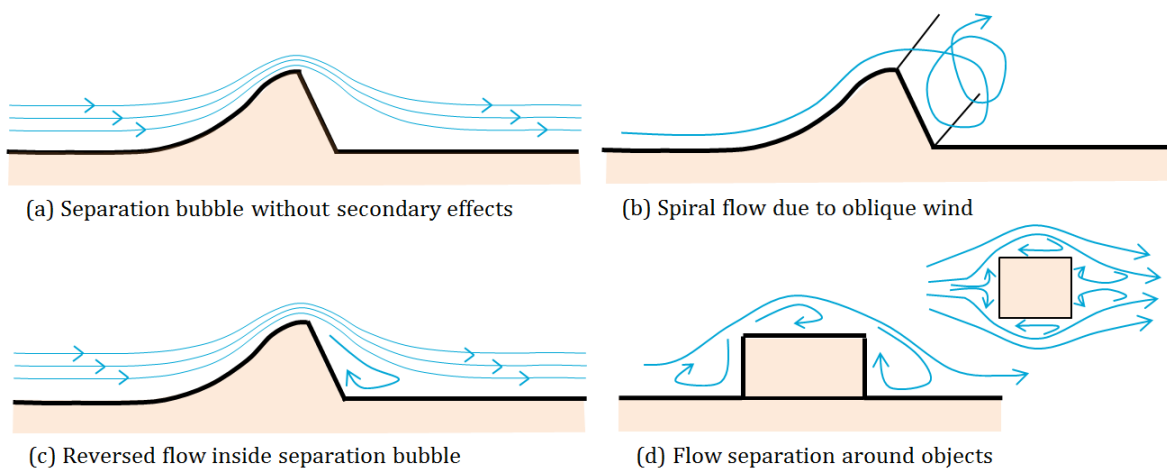


Figure 2.3: Various possible implementations methods of the separation bubble

2.1.3. Avalanching

When slopes become too steep, avalanches sets the sand surface to the angle of repose. This could be the result of erosion by hydrodynamic processes, stabilization by vegetation or an increased sediment deposition, for instance just behind the separation of flow.

Avalanching is initiated once the slope becomes steeper than a certain value: The static angle of repose. Once the avalanching process has started, the slope will finally set to a bit steeper angle, which is called the dynamic angle of repose. The value for the angle of repose depends not only on the type of sediment, but also on external conditions such as surface moisture content.

2.1.4. Non-erodible elements

Non-erodible elements are objects or layers which can not erode due to aeolian processes. Examples of such elements are rock or clay layers and human-made objects such as concrete slabs, houses, fences or rocks. These objects can cause local erosion in coastal areas. Since these objects are not smoothed by aeolian processes, flow patterns around objects can become complicated due to the resulting three dimensional flow separation (see figure 2.3 (d)).

2.1.5. Vegetation

The presence of vegetation has a stabilizing effect on dune development. The dune-building species that can be found in coastal areas have unique characteristics that allow them to grow in the dynamic coastal regions with high salinity concentrations. The growth of dune-building species and their influence on coastal dune development can be divided into different processes, see figure 2.4.

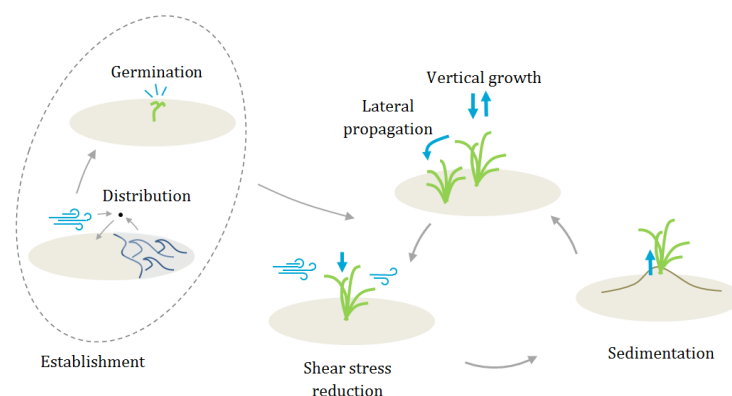


Figure 2.4: Vegetation processes

Vegetation as a roughness element

The presence of vegetation causes a reduction in shear velocity. The reduced shear velocity causes the deposition of sediment, growth of dunes and the burial of vegetation. Raupach et al. (1993) proposed a relation on the effect of vegetation on the effective shear stress.

Vegetation establishment

The process of vegetation establishment consists out of the dispersion and germination of seeds or rhizomes. Dispersion happens under the influence of aeolian or hydrodynamic processes and therefore establishment of vegetation happens more often near existing vegetation, since the distance seeds or rhizomes have to cover is shorter. The germination of a seed depends on numerous conditions, such as anthropomorphic activity, dynamics of the bed level, groundwater table, soil salinity. In the *DUBEVEG* model (Keijsers et al., 2016), the probability of establishment is assumed to be uniform over the entire coastal area. Based on observations along the Dutch coastline the probability of establishment is estimated to be $0.05 / \text{m}^2 / \text{year}$ (Keijsers et al., 2015).

Change in vegetation cover

After the establishment of vegetation, it starts to grow. A unique characteristic of dune-building species is that these are burial tolerant, due to the relative high growing velocity. Besides, during the burial of the vegetation, the micro-environmental characteristics of the soil change. These changes in soil characteristics can drive the growth of typical dune-building species. Therefore dune-building species are not only burial-tolerant, but often growth is stimulated in the situation of sedimentation. [Maun \(2009\)](#) gave a qualitative description of the characteristic response of dune-building species to sediment burial, see figure 2.5.

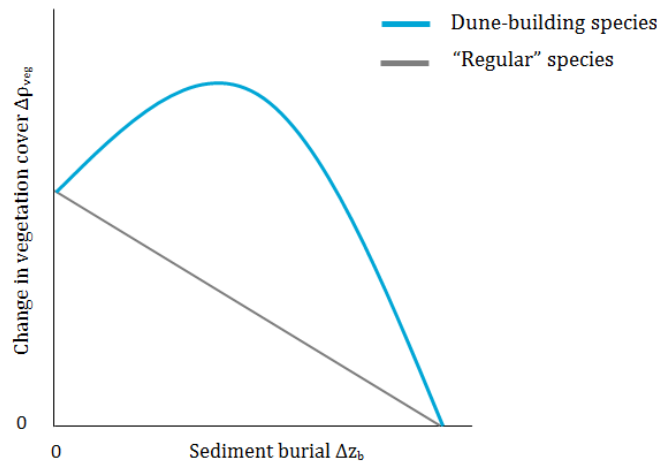


Figure 2.5: Qualitative description of response of vegetation to sediment burial ([Maun, 2009](#)).

Field-measurements from [Nolet et al. \(2017\)](#) confirm this qualitative description. ([Nolet et al., 2017](#)) measured growth of vegetation expressed in changes in NDVI and related it to sediment burial. The measurements were carried out on the foredunes in the domain of the Sand Motor. Due to the height elevation of the chosen location, hydrodynamic storm erosion could not influence the measurements. The results are plotted in figure 2.6.

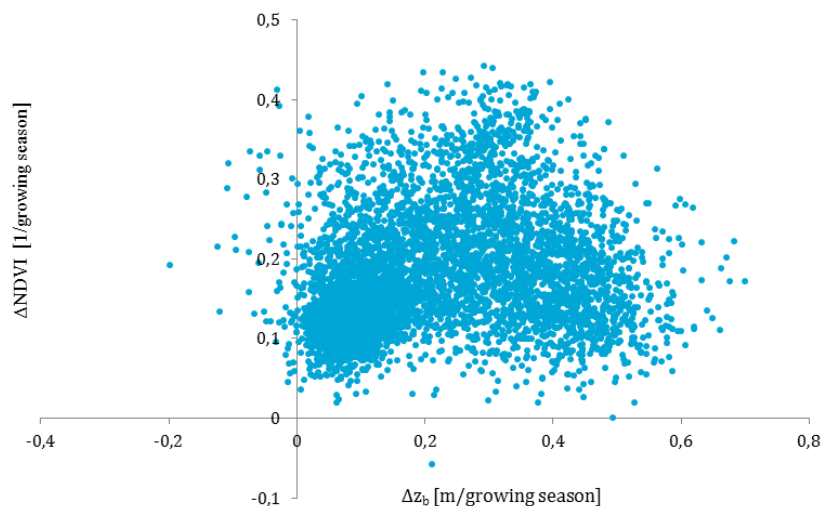


Figure 2.6: Vegetation growth related to sediment burial from April to August 2015, measured at the Sand Motor ([Nolet et al., 2017](#))

Although the measurements compare well with the description from [Maun \(2009\)](#), several remarks have to be made on the measurements. Only the measurement data from the growing season is shown (April - August 2015). Outside of the growing season, hardly any relation between change in vegetation cover and sediment burial can be found. Besides, the interaction between vegetation and sediment burial is a positive feedback mechanism, which are in general hard to capture in measurements.

Current numerical models related to coastal dune development also related the growth of vegetation directly to sediment burial. [Durán and Herrmann \(2006b\)](#) (*CDM*) included the growth of vegetation related to sediment burial in *CDM*:

$$\frac{\delta \rho_{\text{veg}}}{\delta t} = V_{\text{veg}}(1 - \rho_{\text{veg}}) - \frac{\gamma}{H_{\text{veg}}} \left| \frac{\delta z_b}{\delta t} \right| \quad (2.1)$$

where ρ_{veg} [-] is the vegetation cover, V_{veg} [m/year] is the characteristic vegetation growth, γ [-] is the relative influence of sediment burial and H_{veg} [m] is the maximum vegetation height. [Durán and Herrmann \(2006b\)](#) stated that vegetation does not grow under erosive conditions, so $V_{\text{veg}} = 0$ if $\left| \frac{\delta z_b}{\delta t} \right| < 0$. Since the vegetation growth is related to the actual vegetation cover in the *CDM* formulation, the growth of vegetation decays over time. This vegetation growth decay is plotted in figure 2.7 for a situation with ideal growth conditions ($\left| \frac{\delta z_b}{\delta t} \right| = 0$).

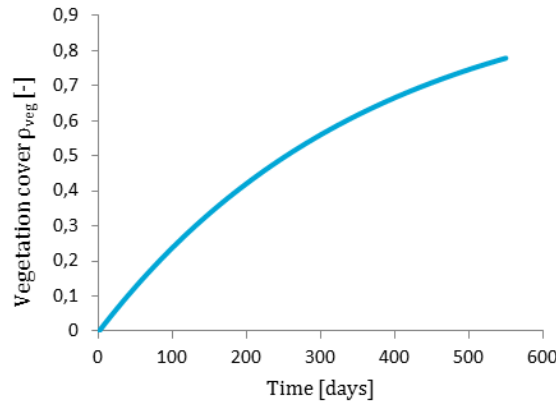


Figure 2.7: Vegetation cover from [Durán and Herrmann \(2006b\)](#) over time with a stable bed.

To be able to compare the solution of the equation with data from [Nolet et al. \(2017\)](#), the measurement data must be converted from NDVI to vegetation cover. Therefore it is assumed that the change in NDVI is proportional to the change in vegetation cover. In figure 2.8, the change in vegetation cover is plotted against sediment burial with $\gamma = 1$, $H_{\text{veg}} = 1$ m and $V_{\text{veg}} = 1$ m/year and for different values of ρ_{veg} . The gray dots indicate the measurement data from [Nolet et al. \(2017\)](#).

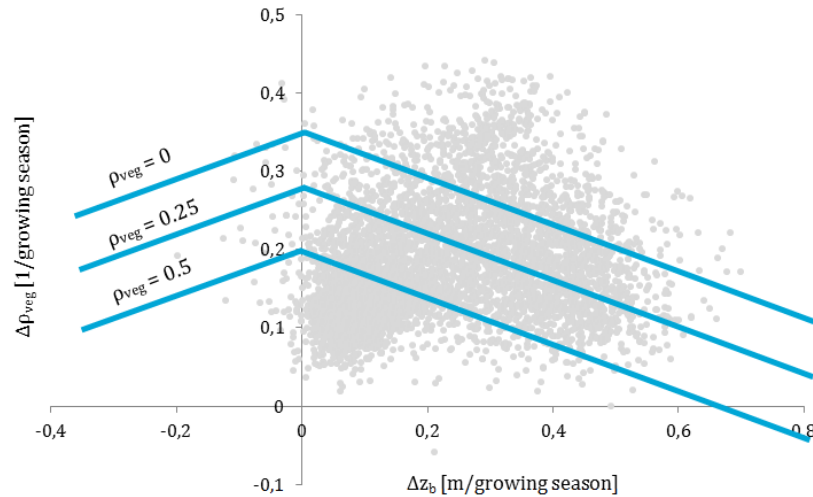


Figure 2.8: Vegetation growth as a result of the formulation from [Durán and Herrmann \(2006b\)](#) for different values of ρ_{veg} , compared with measurement data from ([Nolet et al., 2017](#)).

It can be seen that the change in vegetation cover in *CDM* is optimal for a stable bed ($\left| \frac{\delta z_b}{\delta t} \right| = 0$), which is not fully corresponding with the description from [Maun \(2009\)](#) and the data from [Nolet et al. \(2017\)](#).

In *DUBEVEG* (de Groot et al., 2011) change in vegetation cover is not described by an equation, but by several data points which are derived from measurements. The change of vegetation cover in *DUBEVEG* is represented by a value ρ that is directly related to probabilistic values for erosion and sedimentation, see figure 2.9. Therefore the parameter representing vegetation cover in *DUBEVEG* has no physical meaning and therefore is not directly comparable with the earlier discussed descriptions, due to the fundamental differences in approach.

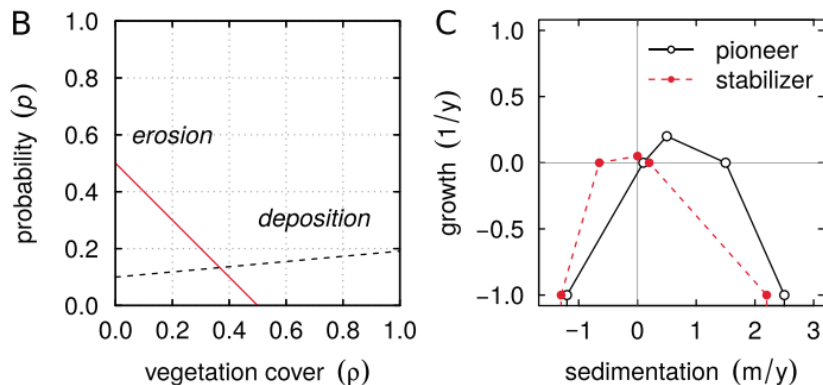


Figure 2.9: Vegetation related to sediment burial in *DUBEVEG*, modified from Keijsers et al. (2016).

In this *DUBEVEG* model, two types of vegetation are modeled: a pioneering species which are burial-tolerant such as marramm grass and a stabilizing species, which is a buckthorn-type vegetation that is more sensitive to bed level changes. Although the method is not quantitatively comparable with the formulation of Durán and Herrmann (2006b) or the measurements from Nolet et al. (2017), it does represent the same behaviour for dune-building species as the qualitative description of Maun (2009).

The discussed method all described vegetation growth based on sediment burial. However, vegetation growth also depends on salinity, anthropogenic influences, meteorology, competition and the availability of nutrients, but these influences are not yet implemented in existing dune development models.

Lateral propagation

Vegetation can expand in lateral direction from existing plants via rhizomes. The ratio between the lateral propagation and local change in vegetation cover has influence on the shape of coastal dunes (Goldstein et al., 2017). Slow lateral vegetation leads to more hummocky dunes, since single plots of vegetation capture the sediment and result in relatively steep hill. Dunes will expand faster in lateral direction in the lateral propagation of vegetation increases, resulting in lower and wider dunes. These type of dunes will quicker coalesce into continuous foredunes.

DUBEVEG describes the lateral propagation of vegetation by a spatially uniform probabilistic variable (Keijsers et al., 2016), similar as for vegetation establishment, but with the restriction that lateral expansion only can occur when a neighboring cell is vegetated. From measurement data (Keijsers, 2015) a probability of $0.2/\text{m}^2/\text{year}$ is determined.

The data from Nolet et al. (2017) can also be used to determine a value for lateral propagation. In order to do so, first it has to be determine if a plot is vegetated or not. Vegetation in a cell is defined as a cell with a NDVI of 0.1 or larger:

$$\text{Cover} = \begin{cases} 1 & \text{NDVI} \geq 0.1 \\ 0 & \text{NDVI} < 0.1 \end{cases} \quad (2.2)$$

Using this definition, it can be determined which cells are vegetated for different moments in time. In figure 2.10 the dark green areas indicate the vegetated cells before the growing season (April) and the light green areas show the vegetated cells after the growing season (August). The blue cells are assumed to be new established vegetation, since there is no connection with existing vegetation before the growing season.

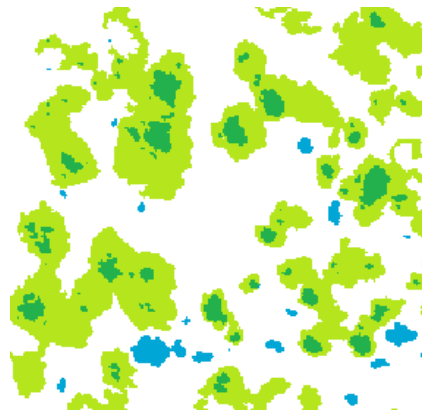


Figure 2.10: Lateral expansion patterns. Dark green: Cover(April). Light green: Δ Cover. Blue: (probably) vegetation establishment through germination. [Nolet et al. \(2017\)](#)

In order to quantify the lateral propagation, polygons are drawn around the different vegetated plots. Subsequently, the area of each polygon is determined, resulting in a characteristic radius obtained by $R = \sqrt{A/\pi}$. The lateral propagation is determined by subtracting the average radius of vegetated plots before and after the growing season. This resulted in a lateral propagation of 0.23 m over the growing season. Assuming that the lateral propagation only occurs during the growing season, the values from *DUBEVEG* and [Nolet et al. \(2017\)](#) compare well.

2.1.6. Marine processes

The marine zone directly influences the sediment budgets by causing erosion and accretion in the nearshore region. In the intertidal zone, marine and aeolian processes interact. Aeolian processes are generally an order of magnitude smaller than marine processes and therefore a beach profile is mainly dominated by marine processes. It is therefore valid to assume that once the hydrodynamics affect an area, the bed level changes as a result of aeolian processes will be smoothed. This means that during calm conditions sediment supply from the marine zone compensates for aeolian transport in the intertidal area, while extreme events can cause the erosion of aeolian dunes, see figure 2.11.

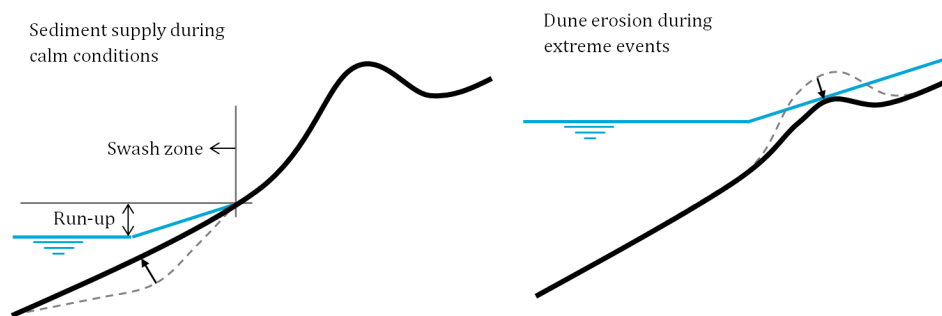


Figure 2.11: Influence of the marine zone during calm conditions and extreme events

The presence of a shoreline also limits the development of coastal vegetation, due to increased salinity concentrations and mechanical erosion. The mechanical erosion of vegetation can occur during extreme events, depending on the water level elevation, wave height and wave strength. Current available numerical models describe the limiting influence of the shoreline on vegetation with a static vegetation limit: A static, user-defined, cross-shore distance between the shoreline and the first line of vegetation ([Durán and Moore, 2013](#); [Keijsers et al., 2016](#)). [van Puijenbroek et al. \(2017c\)](#) stated that models would be more realistic if models use a dynamic instead of a static vegetation limit. Instead of a static distance, the existence of vegetation should be directly related to wave impact and/or salinity concentrations.

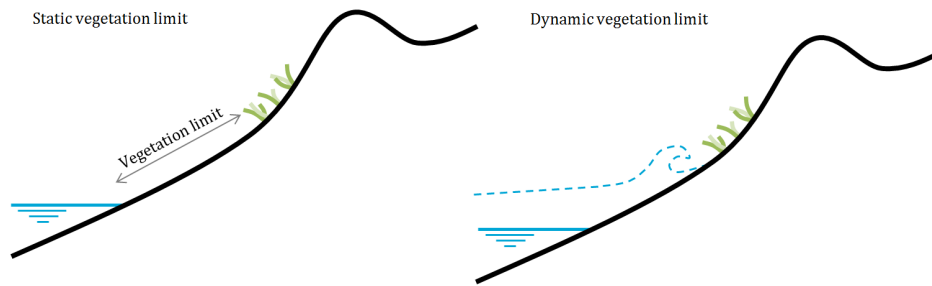


Figure 2.12: Static and dynamic vegetation limit.

Sediment with a increased surface moisture content has a larger velocity threshold, so the presence of a shoreline limits sediment transport. *CDM* and *AeoLiS* have a different approach for the representation of surface moisture, respectively fetch-limited and supply-limited transport, as discussed earlier in section 2.1.1.

Besides a limiting effect on sediment transport, the shoreline can also enhance sediment as a result of the mixing of the top layer (Hoonhout and de Vries, 2016a). Waves cause the mixing of the upper layer of the bed, removing the armour layer (see section 1.1.2).

2.2. Landforms

The shape of a landform depends on external conditions and the influence of related processes. In this section, the development of three landforms will be discussed: Barchan, parabolic and embryo dunes. The processes that are important for the shape will be mentioned and a short overview of the recent research on the landforms will be given.

2.2.1. Barchan dunes

Barchan dunes are formed under limited sediment transport and without the influence of vegetation or the shoreline. The development of a barchan dune will be described based on a initial situation with an isolated pile of sand (Hersen, 2004).

When wind approaches an isolated sand pile, the wind starts accelerating and an erosive trend occurs at the windward side. Due to the separation of flow at the brink line, the wind velocity drops, particles are deposited and consequently the dune starts migrating. The speed of this process migrating process is faster for smaller heights and therefore the sides of the dune move faster than the central part of the body: the horns start to grow. At the central part of the dune, the developed separation bubble causes a steep slope at the slip face. Because of the reversed flow of the separation bubble, particles in the slip face are trapped and there will be no flow downwards of the main body. Avalanches occur when the slope of the slip face exceeds the angle of repose.

In recent years, research has been performed on the shape and development of barchan dunes. Sauer-[mann et al. \(2000\)](#) measured several barchan dunes in the south of Morocco and proposed a simplistic model for the dune shape, see table 2.1. [Sauer-\[mann et al. \\(2003\\)\]\(#\)](#) measured barchan dunes in the northeast of Brazil, showing the invariant character of barchan dune migration and predicted the migration velocity.

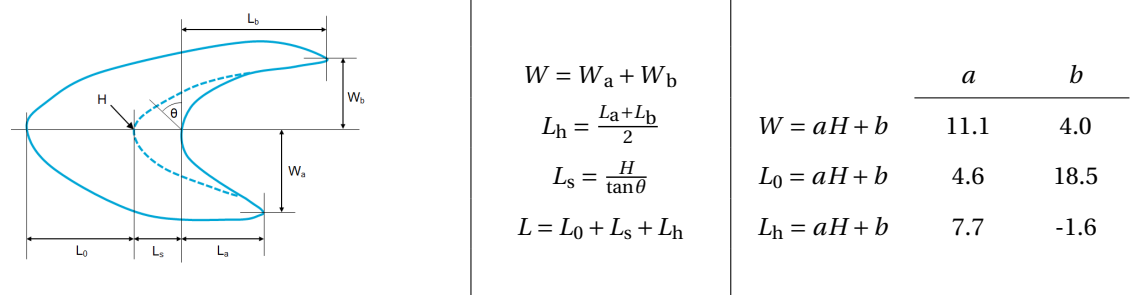


Table 2.1: Dimensions of measured barchan dunes, modified from [Sauer-\[mann et al. \\(2000\\)\]\(#\)](#).

2.2.2. Parabolic dunes

Parabolic dunes are a characteristic landform resulting from the interaction between stabilizing by vegetation, wind fields and morphology. The formation of a parabolic dune will be described by taking a barchan dune as initial topography subject to a unimodal wind. In the initial situation no vegetation is present.

The growth of vegetation is related to sediment burial: Vegetation is not likely to grow in areas that are prone to high erosion or sedimentation. Therefore, the windward side of the barchan will not be grown, because it is subject to a strong erosive trend. In areas with low bed level changes, such as the horns and the brinkline, vegetation is able to grow. As a result the middle part of the barchan will migrate in windward direction, while the horns are stabilized.

In order to quantify the stabilization process of a parabolic dune, [Durán and Herrmann \(2006b\)](#) proposed the fixation index θ (-) which is a dimensionless parameter representing the interaction between sediment transport and vegetation growth:

$$\theta \equiv \frac{Q_0}{V_{\text{dune}}^{1/3} V_{\text{veg}}} \quad (2.3)$$

where Q_0 ($\text{m}^3/\text{m/s}$) is the saturated sediment transport over a flat bed, V_{dune} (m^3) is the volume of the dune and V_{veg} (m/s) is the characteristic vertical growth of the vegetation. A lower fixation parameter θ means a

higher influence of vegetation on the development process. The fixation parameter is related to the inactivation time of a parabolic dune, which is defined as the time required for stopping the migration of the entire dune.

$$t_s \approx \frac{0.17 t_m}{\theta_c - \theta} \quad (2.4)$$

where the characteristic dune migration time $t_m \equiv V^{2/3}/Q_0$ (s) and θ_c is a critical fixation value for which it was found that in situations with a higher θ the vegetation is not able to stabilize the dune.

2.2.3. Embryo dunes

Embryo dunes are the initial stage of coastal dune development. The main difference between the development of parabolic dunes and coastal dunes is the influence of the presence of the shoreline. The shoreline limits the growth of vegetation and causes dune erosion.

[van Puijenbroek \(2017\)](#) explored the boundary conditions for embryo dune development along the Dutch coastline. A positive correlation was found between the beach width and embryo dune development for beaches between 1 - 3 m NAP (Amsterdam Ordnance Datum), which can be explained by the increased aeolian fetch length and a better protection against storm erosion.

While the zonation of embryo dunes is mainly determined by the interaction between morphology and storm erosion, the shape of embryo dunes is largely influenced by vegetation characteristics. The ratio between establishment, change in vegetation cover and lateral propagation determine the "hummockiness" of the dune and the time required before isolated embryo dunes start to coalesce into continuous foredunes ([Goldstein et al., 2017](#)).

[van Puijenbroek et al. \(2017b\)](#) performed field measurements on the shape and growth of embryo dunes. The vegetation cover and bed level on an embryo dune field were measured in August, April and November. These measurements are useful for deriving some parameters on the shape and growth of embryo dunes and characteristics of embryo dune fields.

[van Puijenbroek et al. \(2017b\)](#) defined embryo dunes as areas located 5 cm above an average bed level in a radius of 25 meter. For each dune the maximum dune height and mean dune height are determined. From the embryo dune area, an average radius can be derived, see [figure 2.13](#).

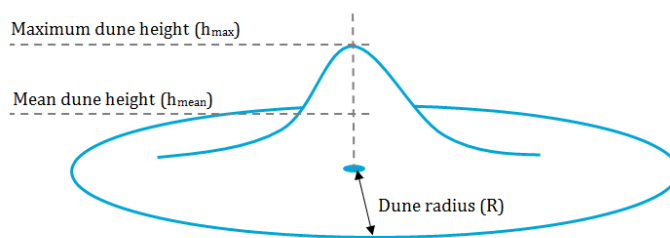


Figure 2.13: Embryo dune dimensions used for validation.

A first characteristic that can be derived from the measurements is the shape of the individual embryo dunes. A characteristic height is defined as the difference between the mean height and the maximum height ($h_{\text{dune}} = h_{\text{max}} - h_{\text{mean}}$). In [figure 2.14](#), the characteristic dune height is plotted against the embryo dune radius, which are obtained from the measurements by [van Puijenbroek et al. \(2017b\)](#).

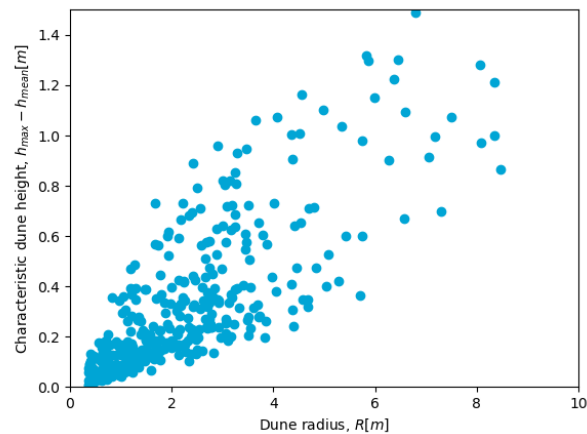


Figure 2.14: Characteristic height of embryo dunes plotted against the dune radius, measurement data obtained from [van Puijenbroek et al. \(2017b\)](#).

Since [van Puijenbroek et al. \(2017b\)](#) performed the measurements in April, August and November, information on the embryo dune growth can be derived for different seasons. The growth of a dune is described by the absolute change in volume. The absolute volume change during the growing season is plotted against the embryo dune radius in figure 2.15.

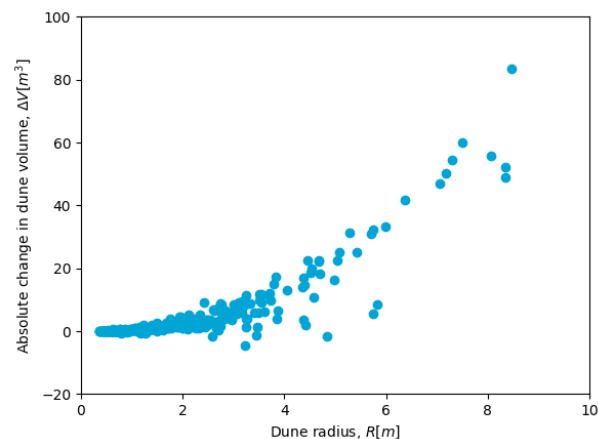


Figure 2.15: Absolute volume change of an embryo dune plotted against the dune radius, data obtained from [van Puijenbroek et al. \(2017b\)](#).

The shape and growth of a dune are characteristics of individual dunes. Since [van Puijenbroek et al. \(2017b\)](#) measured an entire dune field, two characteristics related to embryo dune field development can be derived: The dune size distribution and the inter-dune spacing ([Durán et al., 2011](#)).

The dune size distribution is described by the percentage of the total dune volume distributed over different dune sizes. The inter-dune spacing is defined as the average distance between an embryo dune and the closest neighboring dune. Both characteristics give information on the current development stage of the embryo dune field and the speed of that process. On the basis of these characteristics, different stages of an embryo dune field can be described, see figure 2.16.

At the initial stage of embryo dune field development, the first plants start to establish and embryo dunes start to develop. The inter-dune distance is still large and only small embryo dunes can be observed. Subsequently, more vegetation establish, so more embryo dunes start to develop and the size of existing embryo dunes increases. As a result the inter-dune distance decreases and the dune size distribution widens. Afterwards, dunes start to coalesce, moving and narrowing the dune distribution again and eventually a continuous foredune will develop. The speed of this process depends on several conditions, such as the ratio

between lateral and local vegetation growth, sediment supply and storm erosion. The dune size distribution and inter-dune space distribution from the measurement data by [van Puijenbroek et al. \(2017b\)](#) are shown in figure 2.17.

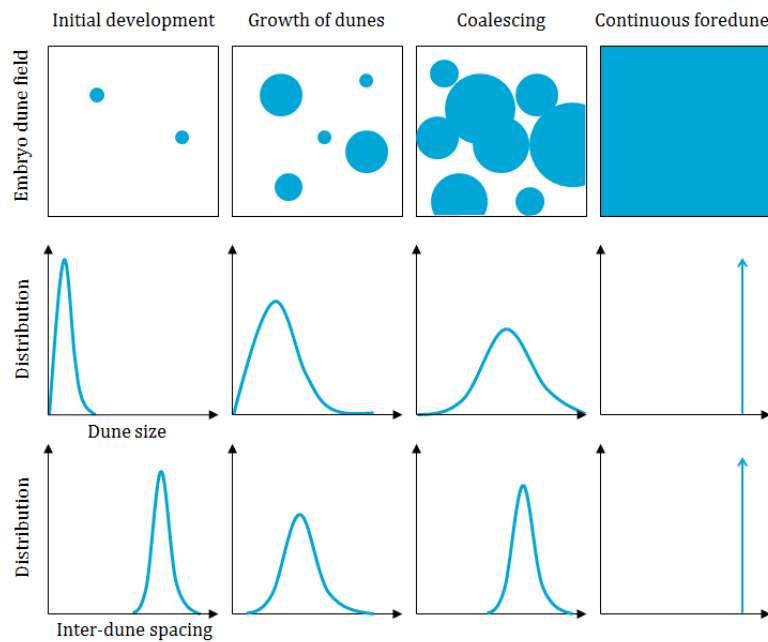


Figure 2.16: Schematisation of the general development of an embryo dune field and the related distributions.

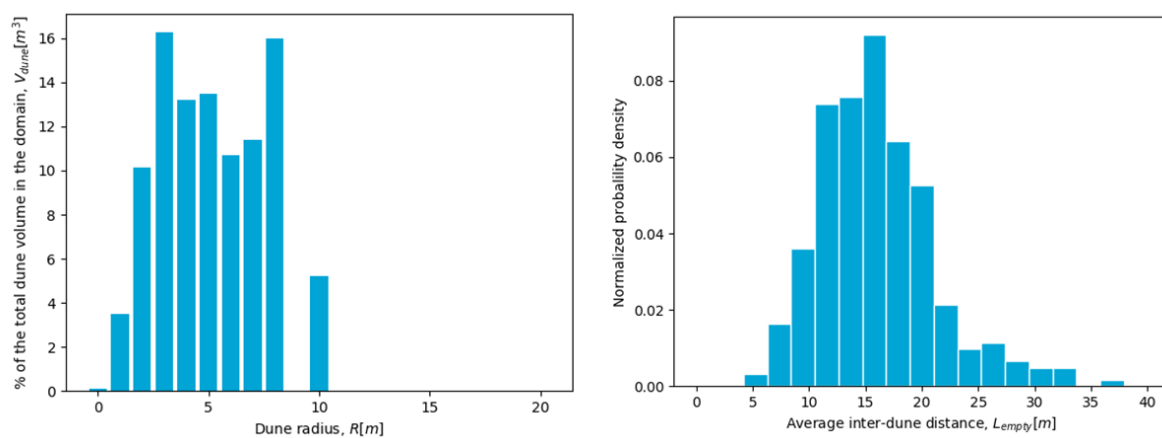


Figure 2.17: Dune size and inter-dune distance distribution, obtained from [van Puijenbroek et al. \(2017b\)](#)

2.2.4. Foredunes

Foredunes are a result of the coalescing of embryo dunes and is a further developed state of the coastal system. In the recent past, the processes behind the foredune development, foredune characteristics and the current numerical model capabilities of simulation foredunes have been researched ([Durán and Moore, 2013](#); [Goldstein and Moore, 2016](#); [Goldstein et al., 2017](#); [Keijsers, 2015](#); [Keijsers et al., 2015 2016](#); [Marco et al., 2011](#); [Moore et al., 2016](#)).

However, discussion is still going on several aspects of foredune development, such as uncertainties concerning the cause of the maximum foredune height, the process behind the auto-cyclical behaviour of foredunes and the influence of the beach width on these characteristics.

2.3. Numerical models related to coastal landforms

Numerical models can be used as a useful tool in the prediction of coastal dune development. Three different models related to aeolian transport, dune development and/or vegetation will be discussed in this section; Coastal Dune Model (*CDM*) (Durán and Moore, 2013), *DUNE-BEACH-VEGETATION* (*DUBEVEG*) (de Groot et al., 2011) and *AeoLiS* (Hoonhout and de Vries, 2016b).

2.3.1. Coastal Dune Model

Kroy et al. (2002) presented a minimal model for aeolian sand dunes *DUNE*, combining a saltation model (Sauermann et al., 2001) and the analytical flow perturbation model (Weng et al., 1991). This analytical flow model describes the spatial varying shear stress as a result of the interaction between morphology and the wind field. Since this theory is only suitable for smooth surfaces, the separation bubble was introduced by Sauermann et al. (2001) to represent flow separation. In the *DUNE* model, it is assumed that the shear velocity is zero inside the separation bubble including the zero shear velocity assumption.

Durán and Herrmann (2006b) included vegetation growth and the influence of vegetation on sediment transport in the model. The local change in vegetation cover is related to sediment burial and the vegetation grows asymptotically towards a maximum user-defined vegetation height. Goldstein et al. (2017) modified the formulation in order to reproduce the sediment burial dependence of dune-building species and added lateral propagation of vegetation. The local change in vegetation cover is linearly proportional to sediment burial and the lateral vegetation growth is related to sediment burial and the difference in vegetation height with the adjacent cells.

Durán and Moore (2013) included effects of the shoreline to the model, changing the *DUNE* model into the Coastal Dune Model (*CDM*). The influence of the shoreline on vegetation growth is described by the implementation of a vegetation limit. Durán and Moore (2013) defined the vegetation limit as the distance between the waterline and the first occurrence of vegetation, which they related to the soil salinity and mechanical erosion. The influence of the shoreline on the velocity threshold is represented by a simple phenomenological expression, relating the velocity threshold directly to the difference between bed elevation and water level. Due to the analytical description of the processes, the method can be categorized as a fetch-limited approach.

CDM is used to simulate a full three-dimensional barchan dune (Schwämmle and Herrmann, 2005). Later, the variation in shape of barchans based on different conditions has been simulated (Parteli et al., 2007), followed by the influence a varying wind strength (Durán et al., 2010) and the development of asymmetric barchan dunes as a result of variation in wind direction (Parteli et al., 2014a). The coalescing of barchan dunes and the formation barchan dune fields has been simulated by Durán et al. (2011). Additionally, the model has been proven to be capable of simulating Martian dunes (Parteli and Herrmann, 2007) and longitudinal dunes (Parteli et al., 2009). Luna et al. (2012) included the influence of an exposed water table in the model.

The implementation of vegetation by Durán and Herrmann (2006b) made the model capable of simulating parabolic dunes. The simulation results of the parabolic dunes showed quantitative good comparison with measured parabolic dunes in Brazil (Durán, 2008). The addition of the shoreline created opportunities for coastal simulations. *CDM* is able to describe some coastal behaviour, such as coastal patterns (Marco et al., 2011), the maximum foredune height (Durán and Moore, 2013) and autocyclic behaviour of foredunes (Moore et al., 2016). Although several observed coastal landforms can be reproduced by *CDM*, there are still several limitations to the model:

- The fetch-limited approach of *CDM* represents an approximation of the time-averaged sediment transport due to transport limiting conditions. This simplification summarizes important processes, such as tidal range, storm frequency, precipitation, infiltration and evaporation into one empirical function.
- *CDM* is not capable of simulating transverse and star dunes. Parteli et al. (2014b) stated that the absence of secondary effects inside the separation bubble could be the cause.
- The vegetation growth formulation by Durán and Herrmann (2006b) describes an optimal vegetation growth in a situation with zero sediment burial, while the growth of certain dune-building species, like marram grasses, are stimulated by sediment burial. The modification by Goldstein et al. (2017) is only suitable for dune-building species, which indicates that the method is not generic, since it is not

compatible with different vegetation species. Besides, the establishment of vegetation by dispersion and germination is missing, so initial dune development such as embryo dunes can not be simulated.

- The influence of the shoreline on vegetation growth is implemented as a user-defined static distance in which vegetation cannot establish. This assumption causes limitations in simulation of coastal dunes, since the influence of dynamic conditions as tides and storms are not included in the model.
- For the simulation of entire coastal areas these processes are essential, so coupling with hydrodynamic models would be favourable. However, because the model is initially developed for academic purposes without considering the future potential of coupling with other models, it is currently hard to couple CDM with hydrodynamic models.

2.3.2. DUBEVEG

Dune-BEach-VEgetation (*DUBEVEG*) is a model presented by [de Groot et al. \(2011\)](#), which simulates dune formation and vegetation succession. *DUBEVEG* combines the dune formation processes from the DECAL algorithm ([Baas, 2002](#)) and vegetation dynamics from the NUCOM model ([van Oene et al., 1999](#)). *DUBEVEG* is a cellular automaton with a probabilistic approach to the formation of dunes and vegetation growth.

Since the approach of *DUBEVEG* is fundamentally different from the intended process-based modelling approach, it is not directly implementable in the new model and therefore the DECAL algorithm behind *DUBEVEG* will not be further discussed in this report. For more information, see [de Groot et al. \(2011\)](#); [Keijsers et al. \(2016\)](#). However, the models approach on vegetation growth is very useful for the development of the new model.

The local growth of biomass is directly related to the sediment burial, see figure 2.9. The germination and distribution is captured into a probabilistic parameter $p_{\text{establish}}$, which is uniform over the entire grid. In reality, an increasing distance from the foredune reduces the dispersion of seeds, so this spatial uniformity is not entirely correct. The lateral propagation of vegetation is also represented by a spatial uniform probabilistic parameter. Once a cell is vegetated, the probability of lateral growth is equal for p_{lateral} for all adjacent cells.

The advantage of *DUBEVEG*'s probabilistic approach is the simplified representation of the complex reality. The development of dunes depends on numerous processes: The establishment of a seed, the occurrence of a storm or tourists passing by. Computing the influence of these processes results in such a complicated situation, it is currently not feasible to simulate these by process-based modelling. Therefore, a probabilistic approach can give a good approximation of reality, which results in an easy to understand and computationally fast model.

The main drawback of the *DUBEVEG* method is that it results in a large dependence on calibration of crucial parameters, limiting the predictive capabilities of the model capable. Additionally, the different approach also complicates the coupling of *DUBEVEG* with process-based, hydrodynamic models. Despite these drawbacks, *DUBEVEG* has been proven to be a useful tool and was able to reproduce embryo (nebkha), barchan and parabolic dunes ([Nield and Baas, 2008](#)) and used to predict dune development in response to climate change ([Keijsers, 2015](#)).

2.3.3. AeoliS

Aeolian sediment transport in coastal areas is generally over-predicted by the existing models ([Sherman and Li, 2012](#)). Supply-limited sediment transport is suggested to be one of the causes of the coastal aeolian sediment transport over-prediction by models. Based on the model approach of [de Vries et al. \(2014\)](#), [Hoonhout and de Vries \(2016b\)](#) presented a model capable of simulating supply-limited sediment transport: *AeoliS*.

The grain size distribution in *AeoliS* is discretized into fractions, which can vary both horizontally and vertically. This makes the simulation of coarse grain sizes sheltering finer particles possible and thus the armoring process can be simulated process-based, rather than through a parameterization of the velocity threshold.

The surface moisture content is related to the velocity threshold and combined with the inclusion of water level elevation, wave run-up, infiltration and evaporation, it gives a process-based description of the shorelines influence on sediment transport. The hydraulic mixing of the top layer is implemented by averaging the sediment distribution in a mixing layer, which depth is related to the breaker height.

The interaction between morphology and wind field is not described in *AeoliS* and therefore the wind field is spatially uniform. As a result *AeoliS* is not capable of simulating dune development.

2.3.4. Overview of processes and models

An overview of all the discussed processes and models is given in table 2.2. The check marks indicate if the process is included in the respective model and the processes with a filled check mark are (partly) implemented in the new model. The letters (a) - (f) redirect to the subquestions in section 1.5.

	Subject	AeoLiS	CDM	DUBEVEG	§
Aeolian processes	(a) Aeolian sediment transport	✓	✓		3.1.1
	Wind fields		✓		3.1.2
	(b) Flow separation		✓		
	(c) Avalanching		✓		3.1.3
	(d) Non-erodible layer		✓		3.1.4
Vegetation	Vegetation as roughness element		✓	✓	3.1.5
	(e) Change vegetation cover ¹		✓	✓	
	Dispersion and germination ¹			✓	
	Lateral propagation ¹		✓	✓	
Marine processes	Swash zone interaction ¹		✓		3.1.6
	(Dynamic) Vegetation Limit ¹		✓		
	(f) Surface moisture content ²	✓	✓		-
	Hydraulic Mixing ²	✓			-

Table 2.2: Overview of dune formation and migration related processes and models

¹ Several processes are difficult to fully implement in a (aeolian) model. Therefore the model is structured such that future coupling with other numerical models is possible.

² See [Hoonhout and de Vries \(2016b\)](#) for more information on the process and [Hoonhout](#) for the background of the implementation in *AeoLiS*.

In this chapter the processes governing coastal dune landforms and the current state of numerical models are discussed. In chapter 3, the implementation of the processes into the new model and the model configuration for the simulation of barchan, parabolic and embryo dunes will be described.

3

Method

The main objective of this thesis is to develop a model that is capable of simulating barchan, parabolic and embryo dunes. In this chapter the technical background of the implementation methods of the required processes will be discussed. Afterwards, a description will be given on the simulation of the landforms that will be simulated with the model, including the related model configuration.

3.1. Implementation of processes

In order to make the model capable of the simulation of landforms, several processes related to dune development have to be implemented. These implementation methods can originate from the existing numerical models *CDM*, *DUBEVEG* and *AeoLiS* or could be based on a new approach. The implementation of each process will be described on the basis of used formulations in the model. A conceptual scheme of the model is shown in appendix A.

3.1.1. Aeolian sediment transport

An advection scheme will be adopted in order to compute the sediment transport. Both *AeoLiS* (eq. 3.1) and *CDM* (eq. 3.2) have implemented an advection scheme:

$$\text{AeoLiS: } \frac{\delta c}{\delta t} + u_s \frac{\delta c}{\delta x} = \frac{c_s - c}{T} \quad (3.1)$$

$$\text{CDM: } \frac{\delta(cu_s)}{\delta x} = \frac{c}{T} \left(1 - \frac{c}{c_s} \right) \quad (3.2)$$

where c (kg/m²) is the actual sediment concentration, u_s (m/s) is the grain speed, c_{sat} (kg/m²) is the saturated sediment concentration and T (s) is the adaptation time scale. The differences between the two schemes are summarized below:

- The advection scheme of *CDM* is based on the assumption of a steady state solution ($\delta c / \delta t = 0$), which is not the case for *AeoLiS*. The exact consequences of this assumption are currently not investigated.
- The velocity in the advection term is a spatially varying grain speed in *CDM*. In *AeoLiS* the grain speed is assumed to be linearly proportional to the wind velocity and since interaction between morphology and wind are not described in *AeoLiS*, the grain speed is spatially uniform. As a result the velocity term is outside of the advection term in *AeoLiS*.
- The formulation of the right-hand side of the equation (net entrainment of sediment) differs in the advection schemes.

For more information on the differences between the advection schemes in *AeoLiS* and *CDM*, see appendix B.

In the new model the advection scheme from *AeoLiS* is chosen, since the consequences of the steady state assumption in *CDM* are not clear and for other programming reasons. For the computation of the parameters within the advection equation (u_s , c_{sat} and T) the formulations in *CDM* are used. In this section an overview of the implemented formulations is given.

A one-dimensional version of the implemented advection scheme reads (de Vries et al., 2014; Hoonhout and de Vries, 2016b):

$$\frac{\delta c}{\delta t} + u_s \frac{\delta c}{\delta x} = E - D \quad (3.3)$$

where $E - D$ represents the net entrainment. The net entrainment $E - D$ is determined based on a balance between the saturated sediment concentration and the actual sediment transport concentration and is maximized by the available sediment in the bed m_a (kg/m^2) (Hoonhout and de Vries, 2016b):

$$E - D = \min\left(\frac{\delta m_a}{\delta t}; \frac{c_{\text{sat}} - c}{T}\right) \quad (3.4)$$

The saturated sediment concentration and time adaption scale are computed following the continuum saltation model by Sauermann et al. (2001):

$$c_{\text{sat}} = \frac{2\alpha}{g} \rho_a \frac{u_*^2 - u_{*th}^2}{u_s} \quad (3.5)$$

$$T = \frac{2\alpha u_s}{g\gamma} \frac{1}{(u_* / u_{*th})^2 - 1} \quad (3.6)$$

where γ (-) is a model parameter account for the splash process.

The grain speed u_s is determined from the momentum balance between the drag force acting on the grains, the momentum loss to the the splashing of grains on the bed and influence of gravity, adapted from Sauermann et al. (2001):

$$\frac{(v_{\text{eff}} - \vec{u}_s) |v_{\text{eff}} - \vec{u}_s|}{u_f^2} - \frac{\vec{u}_s}{2\alpha |\vec{u}_s|} - \vec{\nabla} z_b = 0 \quad (3.7)$$

where v_{eff} (m/s) is the effective wind velocity, u_f (m/s) the grain settling velocity, α (-) represents an effective restitution coefficient and z_b (m) is the bed level elevation. It has to be remarked that u_s is the horizontal movement of sediment in saturated state, not the velocity of individual particles.

In order to compute u_s , equation 3.7 must be solved numerically, but since the slopes occurring have a maximum 34° (dynamic angle of repose), it is assumed that the grain transport direction $\vec{u}_s / |\vec{u}_s|$ can be approximated by the wind direction $\vec{e}_\tau = \vec{u}_* / |\vec{u}_*|$. The grain velocity can be approximated by:

$$\vec{u}_s \approx \left(v_{\text{eff}} - \frac{u_f}{\sqrt{2\alpha A}} \right) \vec{e}_\tau - \frac{\sqrt{2\alpha} u_f}{A} \vec{\nabla} z_b \quad (3.8)$$

where $A \equiv |\vec{e}_\tau + 2\alpha \vec{\nabla} z_b|$. The interaction between the saltation of grains and the airflow in a saltation layer result in an effective wind velocity: The wind effectively action which on the grains. The effective wind velocity v_{eff} is not calculated by using a logarithmic profile, but according to:

$$v_{\text{eff}} \approx \frac{u_{*th}}{\kappa} \left(\ln \frac{z_1}{z_0} + \frac{z_1}{z_m} \left(\frac{\vec{u}_*}{u_{*th}} - 1 \right) \right) \quad (3.9)$$

where u_{*th} (m/s) is the shear velocity threshold, u_* (m/s) is the shear velocity, κ (-) is the Von Kármán parameter, z_1 (m) represents a height within the saltation layer, z_0 (m) is the bed roughness and z_m (m) is the characteristic height of the saltation layer.

The coexistence of multiple sediment fractions can cause sediment sorting, that can lead to beach armouring or the emergence of non-erodible roughness elements (Hoonhout and de Vries, 2016b). Despite the fact that sediment sorting influences the quantitative capabilities of the model, this is not yet fully implemented and therefore the model is not yet suitable for multi-fraction sediment simulations.

3.1.2. Wind field

The interaction between the wind field and morphology is described by the implementation¹ of the analytical perturbation theory for turbulent boundary layer flow (Kroy et al., 2002; Weng et al., 1991). Since the solution is only valid parallel to the wind direction, an overlaying grid is implemented which rotates along with the changing wind direction in time and space.

When considering a small sand heap on the topography $z_b(x, y)$, the velocity profile $\mathbf{v}(x, y, z)$ is calculated by:

$$\vec{v}(x, y, z) = \vec{v}_0(z) + \delta\vec{v}(x, y, z) \quad (3.10)$$

where $\vec{v}_0(z)$ is the unperturbed wind velocity profile. Using the Prandtl turbulent closure, the shear stress can be computed by:

$$\tau = \rho(\kappa z)^2 \left(\frac{\delta v}{\delta z} \right)^2 \quad (3.11)$$

where ρ is the fluid density, $\kappa \approx 0.41$ is the von Kármán constant for turbulent flow and $v(z)$ is the vertical wind profile. The velocity profile $\vec{v}(x, y, z)$ subsequently leads to the surface shear stress $\vec{\tau}(x, y)$ by:

$$\vec{\tau}(x, y) = \vec{\tau}_0 + |\vec{\tau}_0| \delta\vec{\tau}(x, y) \quad (3.12)$$

where $\delta\vec{\tau}(x, y)$ is the shear stress perturbation. The subscript 0 indicates the mean values on a flat bed. The shear stress perturbation $\delta\vec{\tau}$ is computed in Fourier space:

$$\delta\vec{\tau}_x(\vec{k}) = \frac{2\tilde{z}_b(\vec{k})}{U^2(l)} \frac{k_x^2}{|\vec{k}|} \left\{ -1 + \left(2\ln \frac{l}{z'_0} + \frac{|k|^2}{k_x^2} \right) \sigma \frac{K_1(2\sigma)}{K_0(2\sigma)} \right\} \quad (3.13)$$

$$\delta\vec{\tau}_y(\vec{k}) = \frac{2\tilde{z}_b(\vec{k})}{U^2(l)} \frac{k_x k_y}{|\vec{k}|} 2\sqrt{2}\sigma K_1(2\sqrt{2}\sigma) \quad (3.14)$$

$$\sigma = \sqrt{iLk_x z'_0 / l} \quad (3.15)$$

where $\tilde{\cdot}$ indicates the Fourier-transformed components of the parameters, k_x and k_y are the components of the wave vector \vec{k} in Fourier space and K_0 and K_1 are modified Bessel functions. The constant $U(l)$ is the dimensionless vertical velocity profile at height l :

$$U(l) \equiv \frac{\ln \frac{l}{z'_0}}{\ln \frac{z_m}{z'_0}} \quad (3.16)$$

where l is the depth of the inner layer of flow and z_m is the height of the middle layer. Both are computed from implicit equations:

$$l = \frac{2\kappa^2 L}{\ln \frac{l}{z'_0}} \quad (3.17)$$

$$z_m = \sqrt{\frac{L^2}{\ln \frac{z_m}{z'_0}}} \quad (3.18)$$

where L is the typical length scale of the hill, which is defined as the mean wavelength of the Fourier representation of the height profile:

$$L \equiv \frac{\int_0^\infty d\vec{k} |\tilde{z}_b(\vec{k})|}{\int_0^\infty d\vec{k} k_x |\tilde{z}_b(\vec{k})|} \quad (3.19)$$

¹The implementation of the analytical perturbation theory has been carried out by Prof. dr. ir. Pieter Rauwoens from KU Leuven

Separation bubble

The separation of flow over sharp edges is represented by the implementation of a separation bubble (Sauer-mann et al., 2001). For each slice in y -direction (parallel to the direction of the wind), the surface of the separation bubble z_{sep} represents the separating streamline shape and has to connect to the bed level z_b . The separation bubble is modelled by a third-order polynomial. The dimensions of the separation bubble are shown in 3.1. The height at brinkline is defined by $z_b(x_{\text{brink}}) \equiv z_{\text{brink}}$.

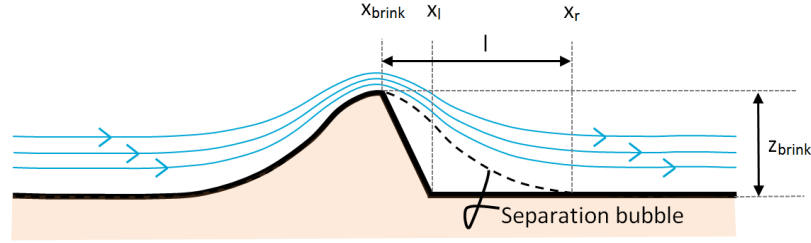


Figure 3.1: Dimensions of the separation bubble

The coefficients of the polynomial are defined by the following conditions:

- Continuity at the brinkline: $z_{\text{sep}}(x_{\text{brink}}) = z_{\text{brink}}$.
- Continuity at of the first derivatives at the brinkline: $z'_{\text{sep}}(x_{\text{brink}}) = z'_{\text{brink}}$
- Smooth conditions at the re-attachment line: $x_r - z_{\text{sep}}(x_r) = 0$ and $z'_{\text{sep}}(x_r) = 0$.

Assuming a maximum slope c for the separation surface, the reattachment length l is obtained by

$$l \approx \frac{3z_{\text{brink}}}{2c} \left(1 + \frac{z_{\text{brink}}}{4c} + 2 \left(\frac{z_{\text{brink}}}{4c} \right)^2 \right) \quad (3.20)$$

The separation bubble z_{sep} is calculated as:

$$z_{\text{sep}}(x) = a_3(x - x_{\text{brink}})^3 + a_2(x - x_{\text{brink}})^2 + z'_{\text{brink}}(x - x_{\text{brink}}) + z_{\text{brink}} \quad (3.21)$$

where:

$$a_2 = -\frac{3z_{\text{brink}} + 2z'_{\text{brink}}l}{l^2} \quad (3.22)$$

$$a_3 = \frac{2z_{\text{brink}} + z'_{\text{brink}}l}{l^3} \quad (3.23)$$

The effect of flow separation on the shear stress is computed by

$$\tau = \begin{cases} \tau & \text{if } z_b \geq z_{\text{sep}} \\ 0 & \text{if } z_b < z_{\text{sep}} \end{cases} \quad (3.24)$$

3.1.3. Avalanching

If slopes are steeper than the static repose angle $\theta_{\text{stat}} (\approx 33^\circ)$ the slope starts avalanching, until the slope will settle down on the dynamic repose angle $\theta_{\text{dyn}} (\approx 34^\circ)$. The sediment transport due to avalanching Q_{ava} is computed by (Kroy et al., 2002):

$$Q_{\text{ava}} = E(\tanh(|\nabla z_b|) - \tanh(\tanh \theta_{\text{dyn}})) \frac{\nabla z_b}{|\nabla z_b|} \quad (3.25)$$

The avalanching method requires two different cell dimensions for the computation: The distance between cell centers and the distance between cell edges. For equidistant computational grids, these distances are equal, but for non-equidistant grids, these distances can differ. To make the avalanching method mass conservative for non-equidistant grids, the coordinates of the computational grid are redefined (Appendix C), following the grid coordinate system in the hydrodynamic model XBeach (Roelvink et al., 2009).

3.1.4. Non-erodible layer

The non-erodability of a layer is processed in the velocity threshold. When the bed level is lower than the user-defined non-erodible layer, the velocity threshold becomes infinitively large:

$$u_{th} = \begin{cases} u_{th} & \text{if } z_b > z_{ne} \\ \infty & \text{if } z_b \leq z_{ne} \end{cases} \quad (3.26)$$

3.1.5. Vegetation

Vegetation as a roughness element

The shear stress acting on the sediment is reduced under the influence of vegetation. With the assumption that the effective shelter area of vegetation is proportional to its basal area, the remaining shear stress acting on the sediment τ_s is given by (Raupach et al. (1993)):

$$\tau_s = \frac{1}{1 + \Gamma \rho_{veg}} \quad (3.27)$$

where Γ (=16 species found in coastal areas) is a roughness factor describing the effectiveness of shear stress reduction by the vegetation.

Change vegetation cover

For the change in vegetation cover, a method reproducing the data from Nolet et al. (2017) and the qualitative description from Maun (2009) would increase the predictive capabilities of the model. The method used by DUBEVEG gives a good description for dune-building vegetation growth, however the units are not compatible with the new model and the development of a similar method is outside of the scope of this thesis.

Various (new) methods have been tried, but eventually a modified version of the formulation by Durán and Herrmann (2006b) is chosen. This formulation has been proven to work properly, is relatively easy to implement and the related fixation index θ provides a solid measure for validation.

In this formulation, change of vegetation cover is related to the sediment burial Δz_b (m/year). A shift of the peak for optimal growth is added to the formulation, in order to represent the sediment burial dependence of various dune-building species:

$$\frac{\Delta h_{veg}}{\Delta t} = V_{veg} \left(1 - \frac{h_{veg}}{H_{veg}} \right) - \gamma \left| \frac{\Delta z_b}{\Delta t} - \Delta z_{b,opt} \right| \quad (3.28)$$

where h_{veg} (-) is the vegetation height, H_{veg} is a constant representing the maximum vegetation height, γ (-) is the sediment burial factor representing the influence of sediment burial on vegetation growth and $\Delta z_{b,opt}$ (m/year) is the sediment burial for optimal vegetation growth. The vegetation cover can be calculated by $\rho_{veg} = \left(\frac{h_{veg}}{H_{veg}} \right)^2$.

Vegetation establishment

The establishment of vegetation is expressed by a probabilistic value $p_{establish}$ (Keijsers, 2015). This probability is equal for all cells in the domain. Once vegetation is established, the vegetation can start growing locally and laterally. If the vegetation dies due to sediment burial or erosion ($\rho_{veg} = 0$), the cell has to get germinated again before vegetation can grow.

Lateral propagation

Similar to the establishment of vegetation, the lateral propagation is represented by a probabilistic value ($p_{lateral}$) equal for all cells adjacent to vegetated cells (Keijsers, 2015). In reality, the lateral propagation is related to the sediment burial and therefore the assumption that $p_{lateral}$ is spatially uniform is not correct. Once lateral propagation has occurred, the local vegetation growth has to be positive, otherwise vegetation dies immediately and lateral propagation has to happen again.

3.1.6. Swash zone interaction

For the description of the hydrodynamic influence on the morphology it is assumed that the beach profile is dominated by the marine zone and that the shoreline is stable. The hydrodynamics relax the beach profile towards initial profile within the area affected by hydrodynamics:

$$\frac{\delta z_b}{\delta t} = \frac{z_{b;0} - z_b}{T_{\text{swash}}} \quad (3.29)$$

where T_{swash} (-) represents a duration timescale for the hydrodynamics to smooth the bed level and prevents numerical instabilities due to sudden changes. The swash zone is defined as the zone where the water level elevation z_s and wave run-up R is larger than the bed level z_b , see figure 3.2. The wave run-up is computed by:

$$R = \xi H_s \left(1 - \min \left(1; \frac{h\gamma}{H_s} \right) \right) \quad (3.30)$$

where ξ is the surf similarity parameter or Iribarren parameter (-), H_s (m) is the significant wave height, h (m) is the water depth ($z_s - z_b$) and γ (-) is the breaker parameter.

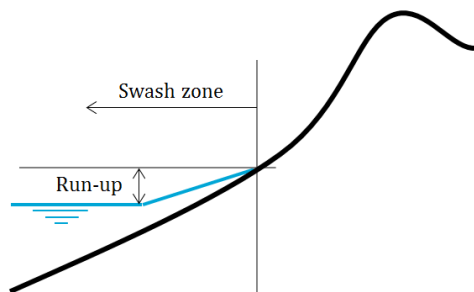


Figure 3.2: Definition of the swash zone.

Under regular conditions, sediment carried away by aeolian processes will be compensated by marine accretion. During extreme events dunes that have developed under the influence of aeolian processes will smooth out, see figure 2.11.

Dynamic vegetation limit

Vegetation dies during extreme weather events under the influence of stresses inserted by waves in combination with the resulting high salinity concentration:

$$\frac{\delta h_{\text{veg}}}{\delta t} = - \frac{\left(\frac{z_s - z_b}{h_{\text{veg}}} \right) H_{\text{veg}}}{T_{\text{dvl}}} \quad (3.31)$$

where T_{dvl} represents a duration timescale for the hydrodynamics to erode the vegetation. It is taken into account that vegetation is less resistant to storm erosion when the vegetation height is still low. This condition is represented by the term $(z_s - z_b) / h_{\text{veg}}$.

3.2. Landform simulation

After the implementation of the processes governing coastal dune development, the simulation of barchan, parabolic and embryo dunes (section 1.5) will be evaluated in this report. In this section the aim and model configuration of each simulation will be discussed. The general model parameters, independent of the simulated landform, are shown in table 3.1.

Parameters			
d	Grain size	0.225	mm
k	Bed roughness	0.01	m
n	Porosity	0.4	-
α	Constant in transport equation	0.4	-
Γ	Vegetation roughness factor	16	-
γ	Gravitational constant	9.81	m/s ²
γ_w	Maximum wave height over depth ratio	0.5	-
θ_{dyn}	Dynamic angle of repose	34	deg
θ_{sep}	Slope of the separation bubble	11	deg
θ_{stat}	Static angle of repose	33	deg
κ	Kármán coefficient	0.41	-
ν	kinematic viscosity of air	1.50E-05	m ² /s
ξ	Surf similarity parameter	0.3	-
ρ_a	Air density	1.225	kg/m ³
ρ_s	Sediment density	2650	kg/m ³

Table 3.1: Overview of general parameters for the landform simulations with the model.

3.2.1. Barchan dunes

Since barchan dunes are a result of aeolian processes without the influence of vegetation and hydrodynamics, it is an ideal landform to evaluate the implementation of aeolian sediment transport, wind fields, avalanching and non-erodible layer. The processes related to hydrodynamics and vegetation are switched off during the barchan dune simulations.

All the barchan simulations will be performed with a sand cone as initial topography. Conditions such as sediment influx, wind velocity and the initial volume influence the shape of the barchan dune and therefore response of the shape of the barchan dune to the variation of these conditions will be shown by simulating under different conditions. An overview of the model configuration for the simulation of barchan dunes is shown in table 3.2.

3.2.2. Parabolic dunes

Parabolic dunes are a result of stabilization by vegetation. Besides the influence of vegetation, the model configuration is the same as for the barchan dune simulations. Therefore, the parabolic dune is an ideal landform to evaluate the influence of various vegetation parameters on the shape of the landform, such as the ratio between wind velocity, dune volume and vegetation growth (fixation index θ , see section 2.2.2) and the shift in optimal growth $\Delta z_{b,\text{opt}}$. The vegetation parameters are chosen in order to obtain a realistic value for the fixation index ($\theta \approx 0.25$). An overview of the parabolic dune simulation configuration is shown in table 3.3.

Barchan dune			
n_x	Cells in x-direction	400	-
n_y	Cells in y-direction	200	-
Δx	Cell size in x-direction	1	m
Δy	Cell size in y-direction	1	m
Δt	Time step	3600	s
Initial conditions			
$z_{b,0}$	Initial topography	Cone	m
z_{ne}	Non-erodible layer	0	m
Boundary conditions			
f_{Q_0}	Factor for relative sediment input	0.18	-
u_w	Measured wind velocity	6	m/s
u_{dir}	Wind direction (nautical)	270	deg
H_s	Wave height	0	m
z_s	Water level	0	m

Table 3.2: Overview of the parameters for the simulation of barchan dunes.

Parabolic dune			
n_x	Cells in x-direction	400	-
n_y	Cells in y-direction	200	-
Δx	Cell size in x-direction	1	m
Δy	Cell size in y-direction	1	m
Δt	Time step	1800	s
Initial conditions			
$z_{b,0}$	Initial topography	Barchan	m
z_{ne}	Non-erodible layer	0	m
Boundary conditions			
f_{Q_0}	Factor for relative sediment input	0	-
u_w	Wind velocity	6	m/s
u_{dir}	Wind direction (nautical)	270	deg
H_s	Wave height	0	m
z_s	Water level	0	m
Vegetation parameters			
$p_{establish}$	Probability of vegetation establishment	1	-
$p_{lateral}$	Probability of lateral propagation to adjacent cell	0	-
V_{veg}	Characteristic vegetation growth	12	m/s
γ_{veg}	Constant on influence of sediment burial	1	-
$\Delta z_{b,opt}$	Shift of optimum growth peak	0	m/year

Table 3.3: Overview of the parameters for the simulation of parabolic dunes.

3.2.3. Embryo dunes

The aim of the simulation of embryo dune fields is to get a better understanding on the influence of different processes on embryo dune development and to see if the model results show comparable behaviour as measured in the field (Goldstein et al., 2017; van Puijenbroek et al., 2017ab).

There are a few differences between the embryo dunes and the barchan and parabolic dunes. Barchan and parabolic dunes are a more academic kind of landform, that have a very characteristic shape, but do not occur very often in reality. The shape of embryo dunes is less characteristic, but can be found more often along coastlines and is easier to measure entire fields instead of one single dune. Therefore, during the simulation of embryo dunes the focus will not only be on the shape and development of a single dune, but also of the distribution of multiple dunes and their location in a embryo dune field.

One aspect of barchan and parabolic dunes is clearly academic is the wind direction that is constant over time. Since embryo dunes are a more practical landform, more realistic wind input is going to be used. It has been tried to simulate with realistic wind velocities and directions obtained from measurements, but instabilities encountered at the boundary, negatively influencing the results. Therefore, the wind velocity and direction are randomly generated with a upper and lower limit ($u_w = 3 - 8$ m/s and $u_{dir} = 225^\circ - 315^\circ$).

The waves and water level elevation are obtained from measurements (Hoonhout, 2017). The topography is a 'regular' beach profile with a slope of 1:50 and it is assumed that the groundwater table, which acts as a non-erodible layer, is located directly under the initial profile ($z_{b,0}$).

The model is not yet capable of simulating conditions that can occur during the storm season, because the implementation of meteorological and hydrodynamic influences on dune erosion and vegetation growth is not sufficient. Therefore, the simulations are based on growing season conditions and it is assumed that the volume change and vegetation growth or decay are negligible during storm season. Assuming that the storm season takes approximately 4 months, a simulation of 1 year is the equivalent of 3 growing seasons.

In order to compare the simulation results with the measurements from van Puijenbroek et al. (2017b), these measurements need to be filtered. Therefore all the measurements outside the growing season are filtered out. Besides, the measured embryo dunes are divided based on an area that was sheltered by a foredune and an area that was directly exposed to the sea. Since no foredune is present in the simulation, the dunes situated behind the foredune are filtered out of the measurement data.

Embryo dune			
n_x	Cells in x-direction	300	-
n_y	Cells in y-direction	100	-
Δx	Cell size in x-direction	1	m
Δy	Cell size in y-direction	1	m
Δt	Time step	3600	s
Initial conditions			
$z_{b,0}$	Initial topography	Beach	m
z_{ne}	Non-erodible layer	Beach	m
Boundary conditions			
f_{Q_0}	Factor for relative sediment input	0	-
u_w	Wind velocity	3 - 8	m/s
u_{dir}	Wind direction (nautical)	225 - 315	deg
H_s	Wave height	Hoonhout (2017)	m
z_s	Water level	Hoonhout (2017)	m
Vegetation parameters			
$p_{establish}$	Probability of vegetation establishment	0.05	-
$p_{lateral}$	Probability of lateral propagation to adjacent cell	0.25	-
V_{veg}	Characteristic vegetation growth	2	m/s
γ_{veg}	Constant on influence of sediment burial	1	-
$\Delta z_{b,opt}$	Shift of optimum growth peak	0	m/year

Table 3.4: Overview of the parameters for the simulation of embryo dune fields.

4

Results

In this chapter, all simulation results will be discussed and, if available, compared with process or landform descriptions in literature and measurement data. First, the performance of the implemented processes will be evaluated and afterwards the resulting landform shapes will be elaborated.

4.1. Processes

The sequence of processes slightly differs during this section compared to the rest of the report. Aeolian sediment transport will be treated last, since it depends on the wind field perturbation and flow separation.

4.1.1. Wind fields

To evaluate the implemented spatially varying shear stress, the shear stress over one dimensional Gaussian shaped hill will be compared with a analytical solution of the theory. [Kroy et al. \(2002\)](#) solved the perturbation model of [Weng et al. \(1991\)](#) analytically for the flow over a Gaussian hill. In figure 4.1 both the analytical and the numerical results are shown. It can be seen that the solutions do not perfectly fit. At the top of the hill and at the downwind side, the amplitude of the numerical solution is somewhat larger. Besides the phase difference at the top compared to the bed level is larger for the numerical solution.

$$f_G(\xi) = \exp(-\xi^2) \quad (4.1)$$

$$\xi \equiv \frac{x}{L} \quad (4.2)$$

$$L = \sqrt{2}\sigma \quad (4.3)$$

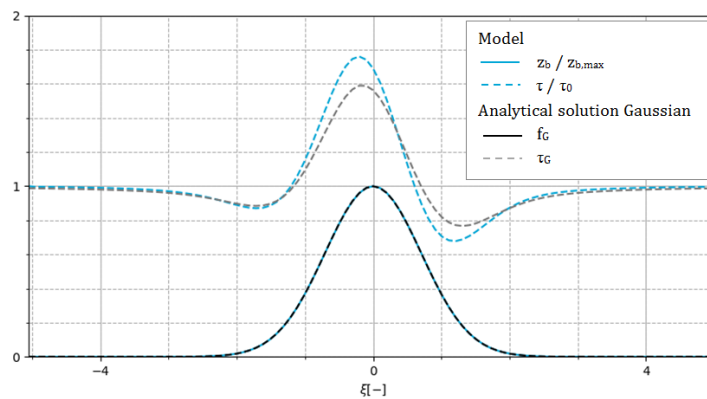


Figure 4.1: Normalized surface shear stress profile over a Gaussian shaped hill from a solution by [Kroy et al. \(2002\)](#) and model simulations.

Flow separation

The influence of the separation bubble on the shear velocity is shown in figure 4.2. The shear velocity is reduced to zero when the separation bubble is larger than the bed level. Around the brinkline a shear velocity peak can be observed, which is probably a result of inaccuracy in the connection between the separation bubble and bed level. This peak and the resulting wiggles can probably be solved by taking a smaller cell size, which was outside of the scope of this thesis due to the currently low computational speed.

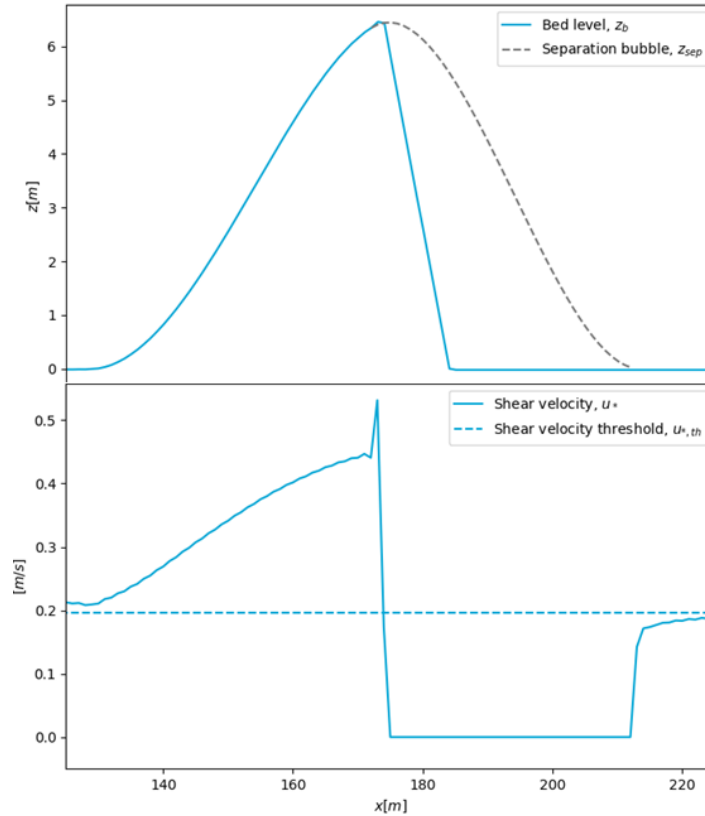


Figure 4.2: A cross-section of the bed level and separation bubble and the resulting shear velocity over a barchan dune.

Shear velocity over barchan dune

The shear stresses over a fully developed barchan dune are shown in figure 4.3. Again, notice the reduced shear velocity inside the separation bubble.

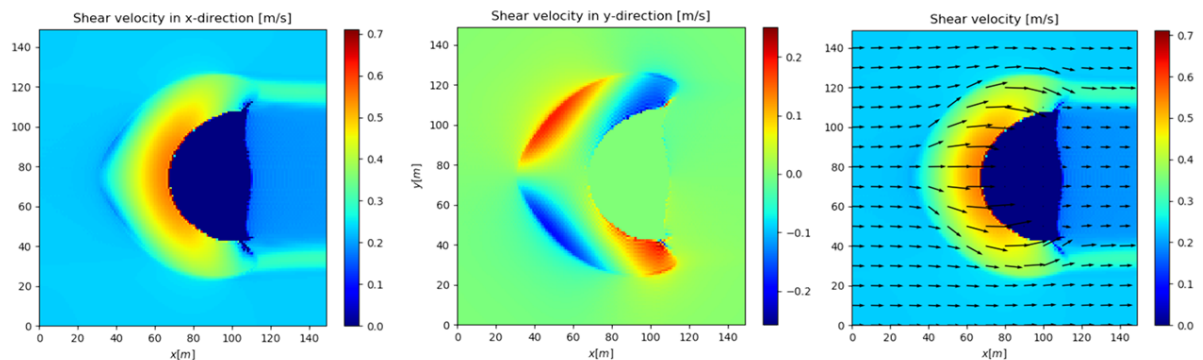


Figure 4.3: The shear stresses in x- and y-direction over a fully developed barchan dune.

4.1.2. Aeolian transport

With the shear velocity known, the sediment transport can be computed. The resulting grain speed is shown in figure 4.4. The sediment concentration is shown in figure 4.5 for three different sediment supplies f_{Q_0} at the incoming boundary ($Q_{in} = f_{Q_0} * Q_0$). In the first situation, with no sediment supply, it can be seen that the sediment concentration at the flat bed and in the separation bubble is zero.

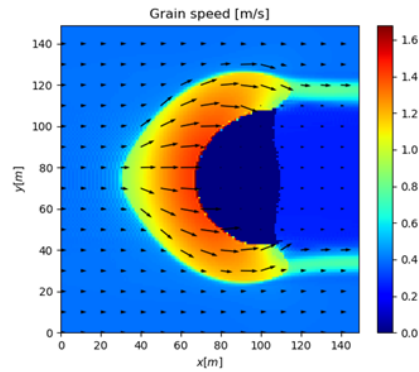


Figure 4.4: The magnitude and direction of the grain velocity over a barchan dune.

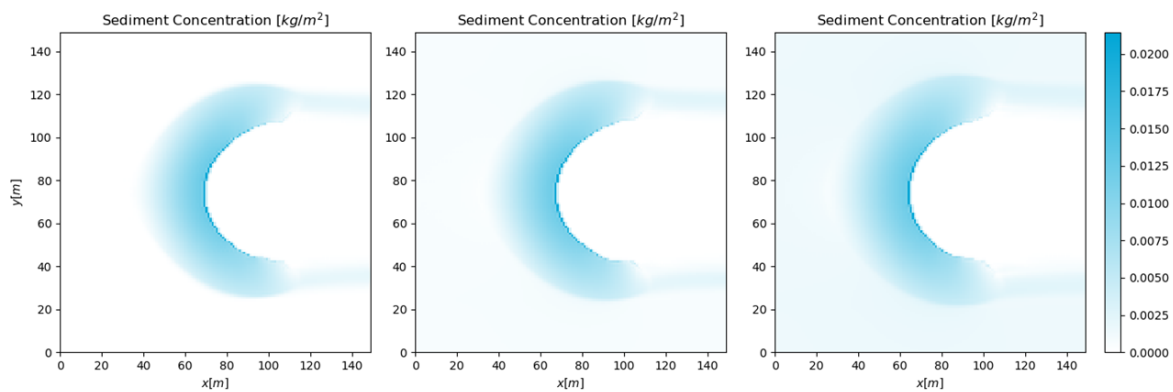


Figure 4.5: Sediment concentration over a barchan dune for a sediment supply of $0Q_0$ (left), $0.18Q_0$ (middle) and $0.36Q_0$ (right).

4.1.3. Avalanching

The avalanching processes relaxes slopes that are too steep towards the angle of repose. However, when the avalanching slope is too large, it takes multiple iterations to solve the entire slope. These iterations can be best shown by the avalanching of a cube. In figure 4.6 the initial state, one intermediate iteration and the final result are shown.

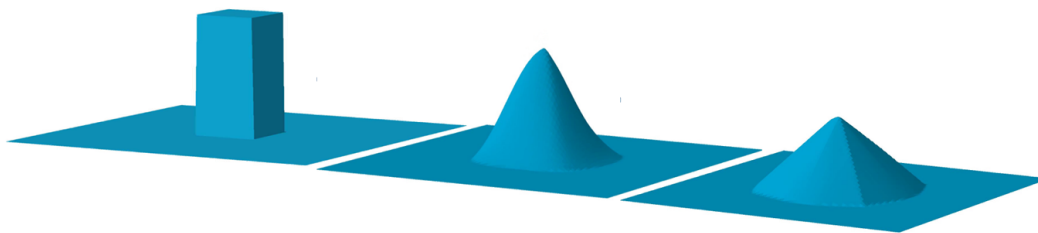


Figure 4.6: Avalanching computation method: The initial state, one intermediate iteration and the final result

4.2. Simulation of landforms

In this section, the development and final shape of the barchan, parabolic and embryo dunes will be simulated. The characteristics of the landforms and the sensitivity to varying conditions will be evaluated.

4.2.1. Barchan dunes

The development of a simulated barchan dune is shown in figure 4.7. Characteristics of this development, such as the speed of the process, migration velocity and equilibrium shape depend on the external conditions. By simulating barchan dunes with varying conditions, the models capabilities of reproducing the expected behaviour can be evaluated.

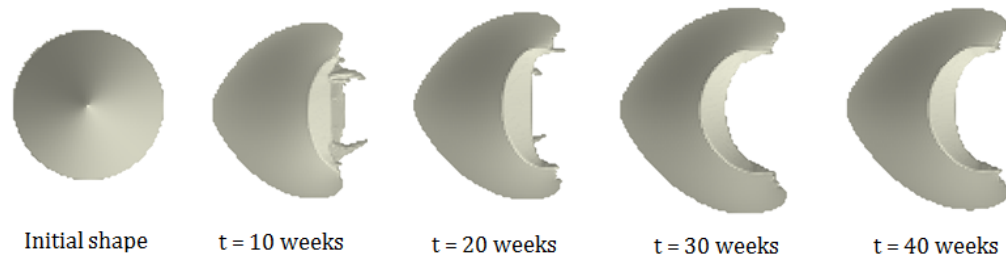


Figure 4.7: The formation of a barchan dune from a cone-shaped initial topography with a wind velocity of 6 m/s.

Migration velocity

Barchan dunes are mobile landforms that migrate in direction of the wind. The migration velocity is a good indicator to check if the model reproduces barchan dune behaviour well. Durán et al. (2010) stated that the migration velocity of a barchans scales with the inverse of the width of the barchan:

$$u_{\text{barchan}} = \alpha \frac{Q_0}{W} \quad (4.4)$$

where $\alpha \approx 50$, which is in agreement with previous studies (Hersen, 2005). For a barchan dune with a width W of 80 m and a wind velocity u_w of 6 m/s, this results in a migration speed of $u_{\text{barchan}} \approx 45$ m/year. From simulations with the model, a barchan under the same conditions migrates with a velocity of approximately 60 m/year.

Wind velocity

The magnitude of the wind velocity influences the equilibrium shape of a barchan dune. A higher wind velocity causes a larger variation of shear stress over the barchan and therefore results in a steeper windward slope. Due to this steeper windward slope, the size of the separation bubble increases and the brinkline is located more towards the windward side. The influence is shown by simulating two barchan dunes, with a wind velocity of respectively 4 and 6 m/s, see figure 4.8.

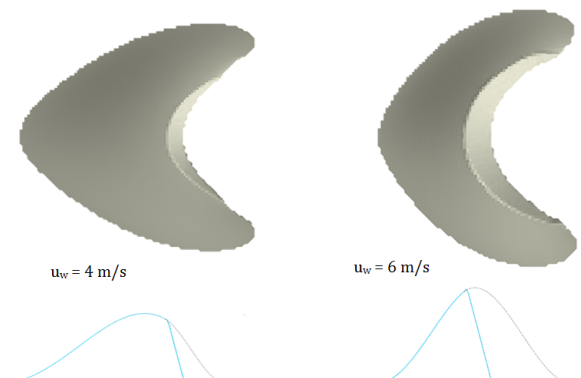


Figure 4.8: Top view and cross-section of a barchan dune under a wind velocity of 4 m/s (left) en 6 m/s (right).

Sediment supply

The sediment supply coming into the domain influences the shape of the dune. When the sediment supply increases, the shape of the windward side gets more rounded and the size of the separation bubble relatively decreases, see figure 4.9.

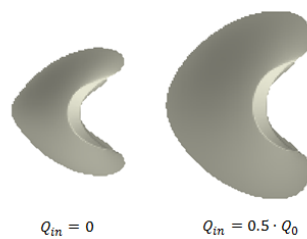


Figure 4.9: The equilibrium barchan shape for two different values for sediment supply.

The volume of a barchan dune depends on the sediment supply and is constant once the sediment transported into the barchan equals the sediment that is transported out. Due to the geometry of the barchan dune and the presence of the separation bubble, the sediment transported out of the barchan dune is all concentrated over the horns. The ratio between the width of the horns and the total width (supply) is approximately 0.18 and therefore the volume of a barchan dune is in equilibrium when $Q_{in} = 0.18Q_0$ (Durán et al. (2010)). In this formulation, Q_{in} is the sediment influx at the boundary and Q_0 is denoted as the saturated flux over a flat bed: $Q \equiv Q_s(u_{*0})$. With a sediment supply lower than $0.18Q_0$, the volume of barchan dunes will decrease over time. This equilibrium sediment supply is well reproduced by the model.

Initial topography

The shape of a barchan dune depends on the initial dune volume, but not on the shape of the initial topography. For decreasing initial volumes, the separation bubble gets relatively smaller (see figure 4.11), until below a certain dune volume the separation bubble completely disappears. That critical volume defines the minimum size of a barchan dune (Parteli et al., 2007).

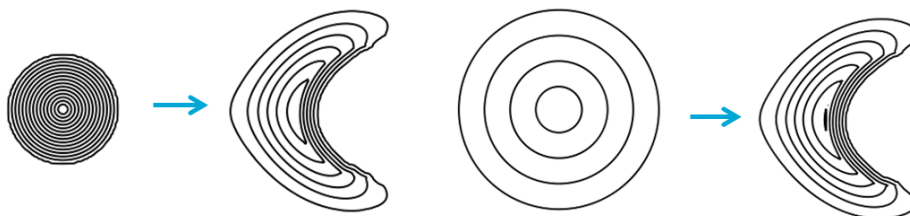


Figure 4.10: The formation of a barchan dune from different shaped initial topographies with approximately the same volume. The height of the topography is indicated with 1 meter contour lines.

The fact that the shape of a barchan dune is independent on the shape of the initial topography, is tested by simulating two barchan dunes from different cone shaped hills with approximately the same volume. The resulting barchan dune is the same for both simulations, see figure 4.10.

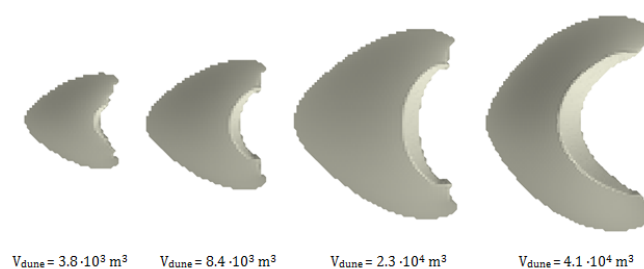


Figure 4.11: The resulting barchans for four different initial volumes.

Measurements of Moroccan barchans

Sauermann et al. (2000) measured eight barchan dunes in the south of Morocco and created relations for some dimensions, linearly related to the height of the dune, see 2.1. Although the amount of measured dunes is limited, the measurements provide a validation with some real world observations.

The wind data in the area is not available. Therefore the wind is assumed to be unimodal and with a constant velocity of 6.7 m/s ($u_* = 0.4$ m/s) (Kroy et al., 2002). The development of the barchan dune is shown in figure 4.12 for a dune volume of 4.1×10^4 m³. On the vertical axis the ratio between the simulated dimensions are divided by the dimensions determined by Sauermann et al. (2000).

It can be seen that the width of the dune is reproduced well by the model, while the length of the horns and the windward slope are too short. These errors could be a result of the uncertainties concerning the advection scheme, the shape of the separation bubble or the processes within that bubble. It can be stated the accuracy of the barchan dunes simulated by the model is good enough for the current state of model development. Once the problems related to the advection scheme and separation bubble are better understood, it is possible to aim for more precise simulations.

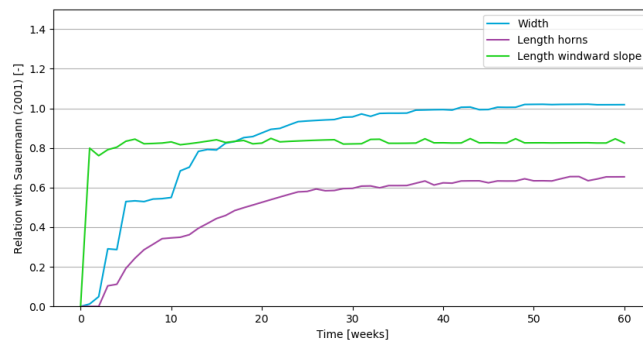


Figure 4.12: The development over time of several barchan dune dimensions, related to measurements obtained by Sauermann et al. (2000).

4.2.2. Parabolic dunes

Similar as for barchan dunes, the validation of parabolic dunes mainly has the objective to validate the influence on dune development of various processes separately. Field measurements are scarce, since parabolic dune development is a long process and hard therefore to measure.

The simulations of parabolic dunes start with an initial hill without the presence of vegetation. Once the simulation starts, vegetation is allowed to grow. Since vegetation growth is negatively affected by erosion and accretion, growth will be maximum at the sides of the dune and thus these areas will stabilize first. While this process continues, the vegetation will grow towards the middle of the dune, until the entire dune is stabilized. The initial stages of parabolic dune development are shown in figure 4.13.

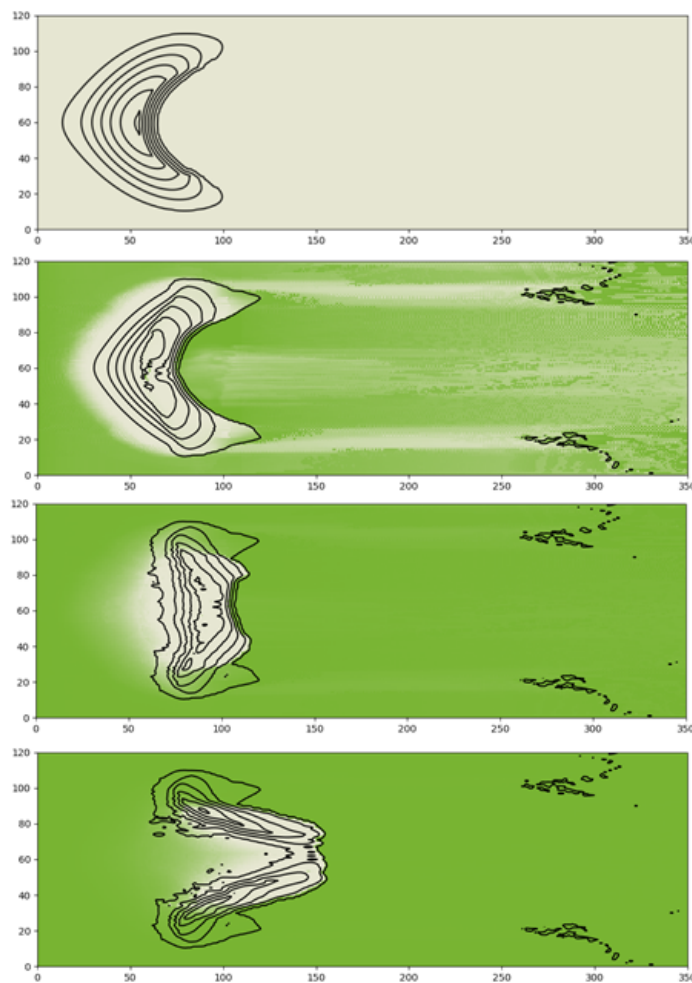


Figure 4.13: Simulation of the development of a parabolic dune, including initial vegetation and stabilization patterns.

Although the initial vegetation and stabilization pattern from the simulation is as expected, the resulting shape of the parabolic dune deviates from simulations done with *CDM*. It seems that the shape of the parabolic dunes heavily depends on some decisions related to the numerical implementation of the separation bubble. Besides, during the simulation the model becomes unstable, leading to increased simulation times and numerical errors causing the simulation to stop. Probably, these problems could be solved by simulating with a finer computational grid, but this is outside of the scope of this thesis.

4.2.3. Embryo dunes

In this section, the models capabilities on the simulation of embryo dunes will be evaluated. The embryo dune field simulations are performed with a model configuration as mentioned in table 3.2.3. The cross-shore distance is in x-direction and the longshore distance in y-direction. The beach profile has a slope of 1:50 and the bed level z_b is 0 m NAP at $x = 0$. Since the mean of the water elevation is approximately 0 m NAP, the cross-shore location of the shoreline is assumed to be at $x = 0$.

In figure 4.14 the bed level changes during the simulation ($z_{b,0} - z_b$) are shown. The general growth pattern is as expected, with initially a few small dunes which start to grow and followed by coalescing. For smaller dunes, behind the embryo dune a "tail" develops along the wind direction, which can also be seen at real-world embryo dune fields.

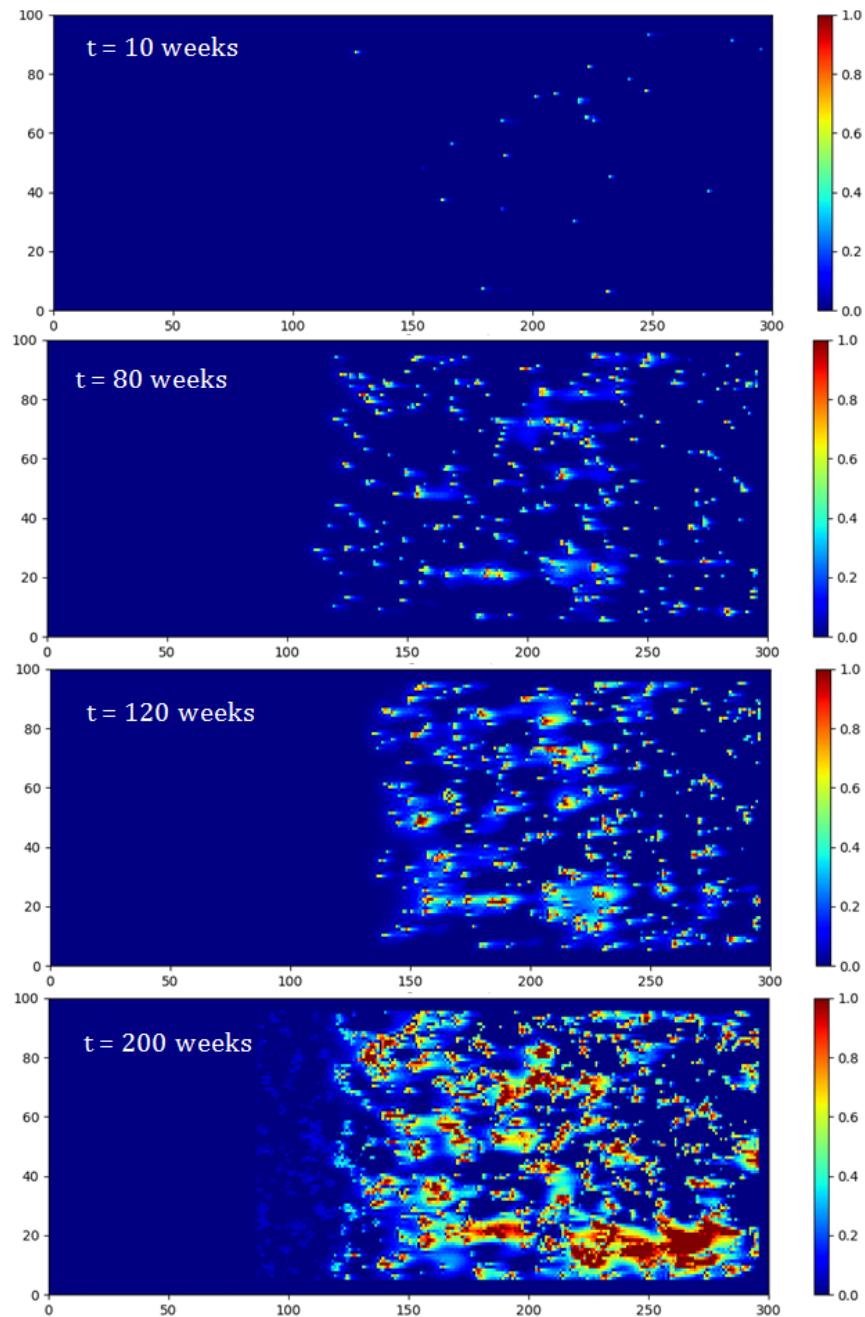


Figure 4.14: Bed level change Δz_b [m] over the simulation of an embryo dune field.

Hydrodynamic influences

The influence of the shoreline on the dune development can be clearly seen from figure 4.14. The cross-shore distance from the shoreline towards the first embryo dune encountered is defined as the length of "empty beach", which varies over time. This temporal variation is shown in figure 4.15.

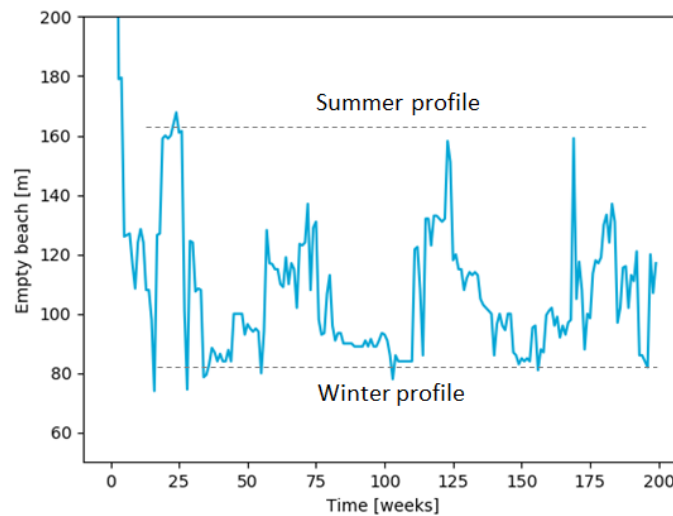


Figure 4.15: Development of the distance from the shoreline to the first encountered embryo dune in cross-shore direction.

The seasonal variation of hydrodynamic influences can be seen in figure 4.15. In a one-year cycle, the embryo dune field grows towards the shoreline and gets eroded during the storm season, resulting in an increased distance between the dunes and the shore. After a continuation of this pattern, the formation of a continuous foredune could be expected in the area that is never affected by the hydrodynamics, approximately 160 m landward in cross-shore direction.

From now on, the analysis on the simulation results will be performed only on the eastern side of the domain ($x > 200$ m), since this part is not affected by hydrodynamics.

Shape of the embryo dunes

In figure 4.16 the characteristic height of an embryo dune is plotted against the dune radius (see figure 2.13) from the model simulations and the data by van Puijenbroek et al. (2017b).

Despite the fact that the measurements from van Puijenbroek et al. (2017b) contain more dunes and that the spread in data is wider, it can be stated that the overall embryo dune shape and the linear proportionality between the both dimensions is reproduced well by the model.

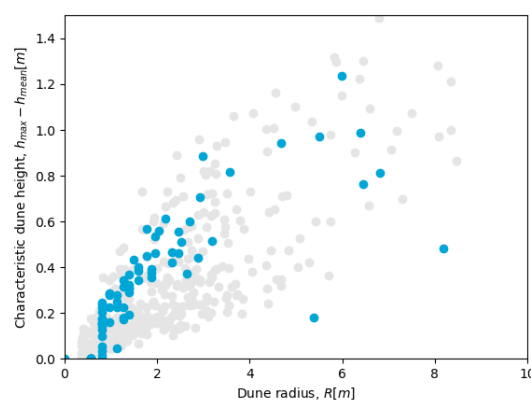


Figure 4.16: Characteristic embryo dune height plotted against dune radius from simulation results (blue) and measurement data (van Puijenbroek et al., 2017b) at $t = 80$ weeks.

Dune growth

The dune growth, expressed in absolute volume change over a growing season (April - August) is plotted against the dune radius in figure 4.17. The order of magnitude of the growth is comparable with the data from van Puijenbroek et al. (2017b).

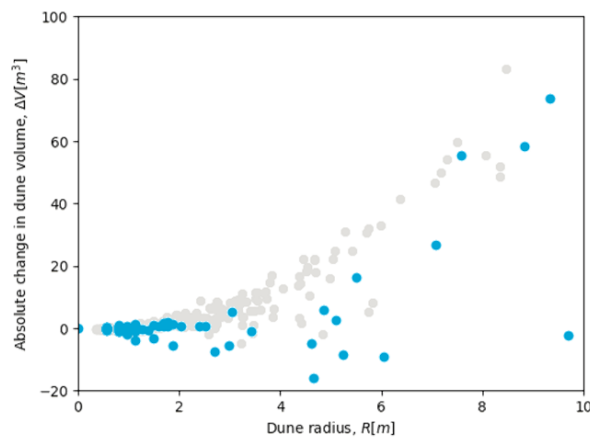


Figure 4.17: Absolute change in volume during one growing season (April - August) plotted against the dune radius for simulation results (blue) and measurements (gray) at $t = 120$ weeks.

Dune size distribution

Goldstein et al. (2017) introduced the term "hummockiness" to characterize embryo dune fields. Every dune field starts hummocky, but as a result of dune growth and coalescing, the embryo dunes will grow into a continuous dune. The hummockiness of a dune field can tell something about the current development stage of the area and speed of the development process.

The speed of this process depends, among other things, on vegetation characteristics. Goldstein et al. (2017) stated that both the lateral vegetation propagation and the change in vegetation cover influence the speed of the development into a continuous foredune. A larger lateral propagation leads to faster coalescing of embryo dunes and therefore increases the development speed towards a continuous foredune. An increased change in vegetation cover results in steeper dunes, since the vegetation is better capable of capturing the sediment, which slows down the development into a continuous foredune.

Based on the shape of the dune size distribution something can be said about the hummockiness of the dune field, see figure 2.16. A decrease in hummockiness is indicated by rightward shift of the distribution.

Several simulations have been performed with three different values for the lateral propagation of vegetation [0.6, 0.25, 0.1] and three different values for the change in vegetation cover [0.5, 2.0, 5.0]. In figure 4.18 and 4.19 the dune size distribution of these simulations are shown. (Note: In order to improve visualization of the results, all the sediment in dunes with a dune radius ($R > 20$ m) is summed up in the last bin ($R = 20$ m)).

For all simulations it can be seen that the distribution shifts towards to right over time, which is as expected. However, also the influence of variation in vegetation characteristics is visible. The development of distribution goes faster for an increased lateral propagation or an decrease in change of vegetation cover.

The dune size distribution from the measurements by van Puijenbroek et al. (2017b) are shown in figure 2.17. Comparison with the dune size distribution from the measurements is difficult, since the distributions change are time dependent. From the dune size spectrum from van Puijenbroek et al. (2017b) it seems that the embryo dunes have grown into "medium-sized" dunes, with little coalescing happening. Once coalescing has occurred, the distribution rapidly shift towards the right. However, it seems that the coalescing happens too fast in simulations with vegetation determined from literature ($V_{veg} = 2$ m/year and $p_{lateral} = 0.25$ /m²/year), since this phase with "medium-sized" dunes are hardly found in the distribution, indicating that the "small-sized" dune rapidly coalesce into a foredune. Using larger values for V_{veg} and smaller for $p_{lateral}$ increases the amount of medium-sized dunes in the distribution.

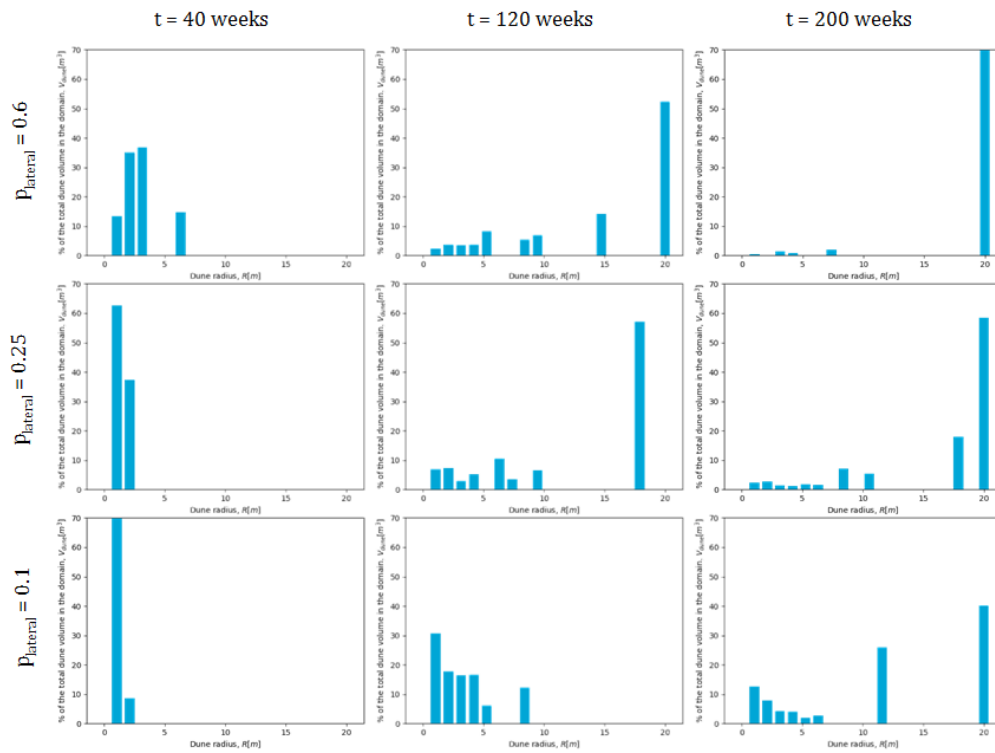


Figure 4.18: Dune size distributions after 40, 120 and 200 weeks for three different values of lateral propagation of vegetation.

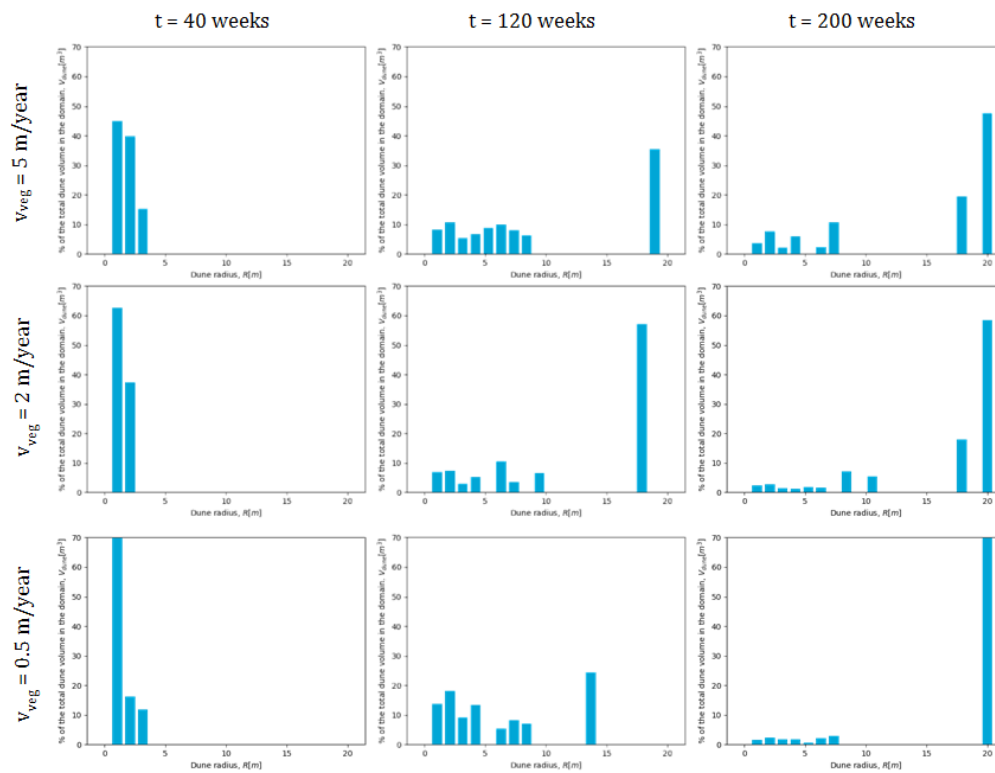


Figure 4.19: Dune size distributions after 40, 120 and 200 weeks for three different values of local change in vegetation cover.

Inter-dune distance

The statement that coalescing with the determined vegetation characteristics happens too fast can be confirmed by comparison of the inter-dune space distributions. The inter-dune distribution of a simulation with $V_{veg} = 2\text{m/year}$ and $p_{lateral} = 0.25$ is shown in figure 4.20.

In comparison with the inter-dune space distribution obtained from the measurements, it can be seen that the overall inter-dune space is larger in the measured dune field (figure 2.17). In conclusion, the currently used vegetation characteristics do not result in a good reproduction of the embryo dune field as measured by van Puijenbroek et al. (2017b). Therefore, values for change in vegetation cover, lateral propagation and establishment (influence of establishment is not analyzed during this thesis) should be reconsidered.

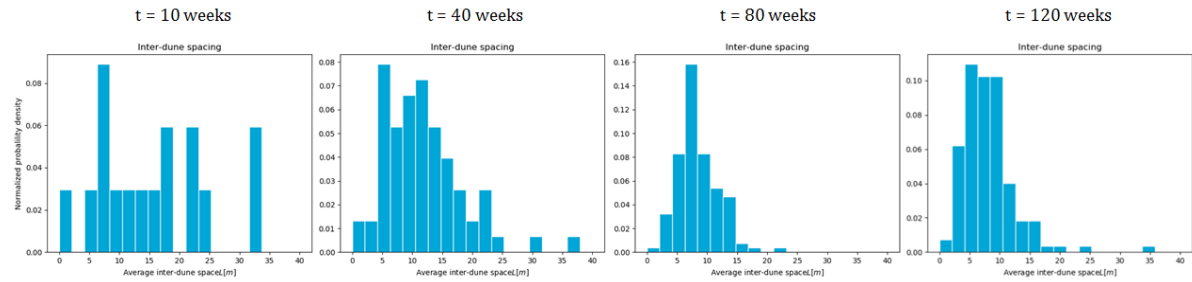


Figure 4.20: Inter-dune space distribution after 10, 40, 80 and 120 weeks.

5

Discussion

Combing the capabilities of several numerical models has contributed to a more process-based description of aeolian, biological and marine processes and potentially a better quantitative prediction of coastal dune development. The most significant contributions in comparison with the current modelling state will be summarized below.

- The combination of a supply-limited approach and the interaction between wind fields and topography is the most significant improvement for the coastal dune modelling state, since it has become possible to simulate dune development with a more realistic approach to sediment transport. Consequently several new situations are potentially reproducible by the model, such as dune development in areas subject to beach armouring and the influence of tidal ranges or storms on the formation and growth of dunes.
- The model is capable of reproducing the establishment and lateral propagation of vegetation due to the addition of a probabilistic approach on germination and lateral expansion. Consequently, the model is capable of describing the formation of embryo dunes and the corresponding characteristics like growth, zonation and coalescing into foredunes.
- The addition of the destruction of vegetation under the influence of water level elevation and wave run-up, a dynamic vegetation limit, is a more realistic approach on the general development of coastal dunes. It is possible to simulate the influence of conditions such as the tidal range, storm intensity, sediment characteristics and beach slope on dune development characteristics, such as zonation, autocyclic behaviour and maximum height.

Although the model development during this thesis has contributed to the process-based modelling of coastal landforms, it must be noted that the model still has a lot of limitations. These can be the result of shortcomings of current implementations or the complete lack of processes.

In this discussion, model-related problems and shortcomings of the implemented processes will be discussed. Afterwards, the influence of these problems on the simulation of landforms will be discussed. This will not only be done for the three simulated landforms (barchan, parabolic and embryo dunes), but also for potential engineering purposes (section 1.1.2).

5.1. Model limitations

5.1.1. Aeolian sediment transport

Advection scheme

In the current state of the model, the most urgent problems are related to the coupling of the two different advection schemes from *CDM* and *AeoLiS*. The main difference between both schemes is the usage of a steady state solution ($\delta c / \delta t = 0$) in *CDM*. For future development of the model it is important that the consequences of this assumption in *CDM* are investigated, because the scheme is much faster than the *AeoLiS* scheme.

Previously CDM has been used (Durán et al., 2011) to perform multi-year simulations of large barchan dune fields. These kind of simulations would take hundreds of days with the current version of the new model. Increased computational speed is therefore essential for the simulation of larger-scale areas, long timescales and a more accurate grid configuration in the model.

The differences between both advection schemes are more elaborately discussed in appendix B.

Multi-fraction sediment transport

AeoLiS is capable of simulating multi-fraction sediment transport. In *AeoLiS* equation 3.4 is modified to make it compatible with multiple sediment fractions:

$$E_k - D_k = \min\left(\frac{\delta m_{a,k}}{\delta t}; \frac{w_k c_{s,k} - c_k}{T}\right) \quad (5.1)$$

where the index k indicates the sediment fraction and w_k (-) a weighing factor. This multi-fraction approach is implemented in the current version of the model.

However, due to the implementation of the continuum saltation model by Sauermann et al. (2001), the grain speed u_s depends on the grain size, since it is related to the shear velocity threshold u_{*th} (see equation 3.9 and 3.7). As a result, the left-hand side of the advection scheme ($\frac{\delta c}{\delta t} + u_s \frac{\delta c}{\delta x}$) also needs to be solved for multiple sediment fractions (equation 5.2). The current version of the model does not solve this side of the advection scheme for different sediment fractions and therefore the model is not yet fully suitable for the simulation of multi-fraction sediment.

$$\frac{\delta c}{\delta t} + \frac{\delta c u_{s,k}}{\delta x} = \min\left(\frac{\delta m_{a,k}}{\delta t}; \frac{w_k c_{s,k} - c_k}{T}\right) \quad (5.2)$$

5.1.2. Wind fields

Flow separation

The current implementation of wind fields is optimized for the formation of barchan dunes and is not fully suitable for the simulation of coastal systems. While dunes in desert areas are fully shaped by aeolian processes, the presence of vegetation and the shoreline can cause irregularities and additional roughness of the bed in coastal areas.

In the model, the starting point of the separation bubble is related to the downward slope: Once a slope approaches the angle of repose, the flow starts to separate. Besides, the shape of the separation bubble in the model is directly related to the topography of the bed. In desert areas, the topography adjusts to the wind field, this assumption is justified, but in the coastal areas the bed has more irregularities.

To get a better representation of flow separation in coastal areas, the initiation of flow separation and shape of the separation bubble should not only be related to the topography of the bed, but should be computed with a more process-based approach, including aeolian characteristics, such as wind velocities and viscosity.

Turbulence, secondary flow and wind gusts

The roughness of coastal areas can increase the amount of turbulence compared to desert areas. Since sediment transport is related to the third power with shear velocity, turbulence can have a significant role in the average sediment transport. The separation of flow has a turbulent character and therefore it is possible that the assumption of zero sediment transport within the separation bubble is not valid for coastal areas. Variations in wind velocity could also be an effect of wind gusts. The current model simulations are computed with time steps in the order of hours, while turbulence effects and wind gusts are in the order of seconds.

5.1.3. Avalanching

The angle of repose in the model is based on dry sand. In coastal regions, the presence of surface moisture content can increase the angle of repose, allowing steeper slopes. In order to increase accuracy, the influence of surface moisture content on the angle of repose should be taken into account, possibly resulting in a spatial variation in angle of repose.

5.1.4. Vegetation

All the aspects of vegetation are represented by very simplified implementations. These simplifications limit the predictive skills of the model. An overview of vegetation-related simplifications that can be solved will be discussed below.

Vegetation growth and sediment burial

The burial of sediment and the growth of vegetation are a feedback mechanism. Vegetation growth is driven by sediment burial and vegetation traps sediment, resulting in larger sediment burial. Results obtained from field measurements are therefore not directly implementable in the model. Future model development should be based on measurements of vegetation growth related sediment burial, while filtering out the capturing affect of vegetation.

More process-based vegetation growth

In reality vegetation growth is not directly driven by sediment burial, but by the altered soil micro-environment caused by sediment burial. Due to sediment burial, temperature, oxygen and light decrease, while moisture, fungi and nutrients increase (Baldwin and Maun, 1983). A more process-based description of vegetation growth based on soil characteristics instead of sediment burial would improvement the predictive skills of the model.

Vegetation competition

Nield and Baas (2008) stated that the shape of a parabolic dune is characteristid by the presence of different species. While vegetation that is highly burial tolerant occupies the lee side of a parabolic dune, vegetation that can survive some erosion is expected to cover the brink. The combination of these types of vegetation causes the rounded shape of parabolic dunes.

With the current implementation in the model, it is only possible to simulate one type of vegetation, reducing the accuracy of the model. Besides, mutual vegetation competition is not implemented, which is could be implemented if one for instance wants to simulate change in biodiversity.

More realistic approach on establishment and lateral propagation

The probabilistic approach on vegetation establishment and lateral propagation results in a randomness of vegetation growth, which contributes to the realistic description of the model. However, the assumption of spatially uniform probabilities does limit the model.

For future versions of the model, it could be considered that the germination probability for cells with dead vegetation is higher, since the remains enhance sedimentation and feed the soil with nutrients. Besides, the uniform character of the approach should be revised, since dispersion does depend on location, such as the distance to the shoreline or the foredune.

The lateral propagation is in reality related to the vegetation cover of the cell it propagates from: It is more likely that vegetation horizontally expands from a plant that is fully grown than from a plant that is just germinated. This is well described by the method introduced by Goldstein et al. (2017), but due to problem related to the calibration of the parameters in the method, it is not implemented. Implementation of this method could improve the predictive capabilities of the model.

Groundwater table and meteorology

Currently, two major aspects of dune development are not implemented in the model: A good representation of the groundwater table and meteorological processes. Meteorology influences vegetation growth directly (for instance sunshine, temperature and snow) and indirectly via the soil moisture content (changes of the groundwater table with precipitation and evaporation). Besides, precipitation and evaporation also influence the threshold velocity of sediment.

During the embryo dune field simulations the groundwater table is assumed to be a static layer slightly below the initial bed level. The inaccuracy caused by this assumption during the simulation of initial dune development is estimated to be small, but since the groundwater table moves along with dune growth, the made error increases over time.

Additionally, the current method lacks the influence of capillary fringe. When water seeps upwards through the pores due to capillary fringe, higher sediment layers can be affected by the increased moisture, which affects the velocity threshold of the sediment. Besides, the emergence of a freshwater lens in a dune can drive the growth of vegetation.

5.1.5. Hydrodynamics

The current implementation of hydrodynamic processes is based on general expected behaviour and is not process-based. Besides, the parameters in the formulation are not calibrated. A full hydrodynamic implementation would induce an unnecessary amount of work, since there are already hydrodynamic models available capable of doing these simulations. The current implementation is kept simple on purpose, since coupling with a hydrodynamic model can overrule the implementation.

The possibility of online coupling with other models is taken into account during the development of the model. Therefore the simulation of complete coastal areas is possible, by combining the interacting processes from marine and aeolian zones. The coupling can improve simulations from an aeolian point of view, such as the formation of dunes, consequences of blow-outs or the development of coastal landforms, because conditions such as surface moisture content, accretion and erosion in the intertidal area and dune erosion during extreme events can be computed more accurately. However, simulations with a marine perspective can also improve due to the coupling, since aeolian transport influences beach and dune profiles.

5.2. Simulation of landforms

Barchan dunes

Although the model simulations of barchan dunes compare reasonably well with simulation with *CDM* and field measurements, there are some small deviations between the results. Example of these deviations are the migration velocity and dimensions of the barchan dune shape. Once it has been proven that the steady state solution from *CDM* ($\delta c / \delta t = 0$) is suitable for the model, the computational speed can increase, allowing simulations with finer grid configurations. It could be possible that an increased accuracy in simulation solves the deviations from *CDM* results.

Parabolic dunes

Similar as for barchan dunes, the problems that occurred during the simulation of parabolic dunes could possibly be solved by increasing the computational speed and therefore allowing the usage of a finer computational grid.

Besides numerical improvements, the implementation of soil characteristic driven vegetation growth, instead of a direct relation with sediment burial, could improve the predictive capability of the model. Additionally, implementing multiple species into the model would improve the shape and development of parabolic dunes as described by [Nield and Baas \(2008\)](#).

Embryo dune fields

The model simulations of embryo dune fields are reasonably well. However, several aspects of the embryo dune development is still described by over-simplified processes. The approach on vegetation establishment and lateral propagation reduce the model's representation of reality. The assumption that these values are spatially uniform is not entirely valid and therefore, to make the model more process-based, the implementation of these vegetation related processes should be extended.

Additionally, the simplifications concerning the description of hydrodynamic processes are justified in the case of a stable shoreline and if one only wants to reproduce some general behaviour of dune development. However, in order to simulate situations with a retreating shoreline or predict the coastal development more accurately, the coupling with a hydrodynamic model is essential.

Engineering purposes

In order to make the model suitable for engineering purposes, the main task again is to investigate if the steady state solution is justified for the model, since this would increase computational speed significantly. Several implementations that need to be improved, added or extended to give the model certain predictive capabilities are meteorology, multi-fraction sediment transport, soil characteristic driven vegetation growth and a more process-based description of the groundwater table should be implemented.

If these processes are implemented, the model should be suitable to be used for engineering problems, such as the emergence of (artificial) blow outs and the effect of armouring on dune development for instance at mega-nourishments. Once the model is coupled with hydrodynamic models, also the response to sea level rise and the recovery of the foredune after extreme events can be simulated.

6

Conclusion

In this thesis, a model has been developed by coupling the capabilities of three different numerical models: *CDM*, *DUBEVEG* and *AeoLiS*. After the implementation of processes that govern coastal landform development, the model capabilities are evaluated by simulating barchan, parabolic and embryo dunes (figure 6.1). This thesis concludes by answering the research questions formulated in section 1.5.

I. Is the model capable of simulating the development of:

A. Barchan dunes

The model is reasonably capable of simulating barchan dunes. Typical behaviour such as the migration velocity, the independence of initial topography and the equilibrium sediment supply are reasonably well reproduced. Besides, variation in shape as a result of different shear velocities, initial volumes and sediment supply are also simulated as expected. Eventually the model results are compared with field measurements. Improvements can be made investigating the problems related to the advection scheme and simulating with finer grid properties.

B. Parabolic dunes

The model is capable of reproducing the expected initial vegetation and stabilization patterns, however the resulting shape of the parabolic dune deviates from simulations done with *CDM*. It seems that the shape of the parabolic dunes heavily depends on some decisions related to the numerical implementation of the separation bubble. Additionally, during simulation the model becomes unstable, leading to increased simulation times and numerical errors causing the simulation to stop. Similar as for the barchan dune, these problems could probably be solved by simulating with a finer computational grid.

C. Embryo dunes

The model is capable of reproducing general characteristics of embryo dune field development. Hydrodynamic influences result in the erosion of vegetation and the smoothing of embryo dunes around the shoreline. For common beach slopes along the Dutch coastline, it seems that the water level elevation and wave run-up during extreme events give a good indication of the location of the first coastal dune row.

The simulated shape of embryo dunes does compare well with measurement data. During the development of an embryo dune field, the dune size distribution and inter-dune space distribution change of time. The transformation of these distributions over time does compare well with the expected development, however using the vegetation characteristics from measurements, the coalescing of dunes in the simulations happens too rapidly compared to measurement data.



Figure 6.1: Overview of the validation landforms during the thesis.

II. How is the development of landforms influenced by the implementation of processes related to:

a. Aeolian sediment transport

The aeolian transport of sediment is the main driver of dune development. The wind starts transporting sediment particles once the wind velocity is higher than the velocity threshold of the grains. This velocity threshold depends on the sediment diameter, but is also affected by the surface moisture content.

The implementation of the aeolian sediment transport in the model is based on a supply-limited approach. The spatial-temporal varying velocity threshold as a result of a process-based description has the potential to improve the predictive capabilities of coastal dune modelling.

b. Wind field

The interaction between the wind field and morphology cause a spatial variation in the wind field. Gradients in wind velocity cause sedimentation and erosion, initiating the development of dunes. The spatial variation of the wind field is described by an analytical flow model, which is only suitable for smooth hills.

In order to make the method suitable for situations where flow separation occurs, a separation bubble is implemented. Within this separation bubble the shear stress is assumed to be zero. As a result of the drop of shear stress, all the sediment immediately gets deposited where the separation bubble starts.

c. Avalanching

Avalanching occurs when a slope exceeds the static angle of repose. Once the avalanching process has started, the slope relaxes towards the dynamic angle of repose. The process of avalanching is implemented as an iterative solver, which distributes sediment towards lower cells once slopes get too steep.

d. Non-erodible elements

Non-erodible elements are objects or layers which can not erode due to aeolian processes. Examples of such elements are rock or clay layers and human-made objects such as concrete slabs, houses, fences or rocks. In the model, presence of a non-erodible element is described by increasing the velocity threshold to infinity.

e. Vegetation

Vegetation acts as a roughness element, resulting in the reduction of shear stress and the deposition of sediment. The establishment of vegetation consists out of the dispersion and germination of seeds and rhizomes. The establishment of vegetation is implemented following a probabilistic approach, with a spatially uniform probability of occurrence.

Once established, vegetation starts growing locally and in lateral direction. A main characteristic of dune-building species is that they are tolerant to sediment burial and moreover, are often driven by sediment burial. The local change in vegetation cover is described by a formulation which relates vegetation growth to sediment burial. The lateral propagation of vegetation is, similar to vegetation establishment, implemented as a spatially uniform probabilistic value.

f. Hydrodynamic

Erosion during extreme events and the marine activity in the intertidal zone are both represented by a function that relaxes the bed towards its initial shape. This approach is only suitable for situations with stable shorelines and the assumption that marine processes are dominant in the intertidal area. Besides, once vegetation is under wave attack, it gets destroyed. This influence of the wave on vegetation is a more dynamic, process-based limitation to the vegetation growth, compared to often used static vegetation limits.

7

Recommendations

Since the development of the model is still in an early stage, a lot of work has to be done before the model can be used as a reliable and practical tool. In order to give a clear overview on all the recommendations and priority of each, the recommendations are separated into several subjects:

- Advection Equation
- Sediment transport
- Vegetation, meteorology and groundwater
- Flow separation
- Coupling with hydrodynamic models

The most urgent problems are related to the advection scheme and will therefore be discussed first. In order to make the model suitable for engineering purposes, the issues related to sediment transport should be solved. The remaining subjects are only relevant in case of more specific cases.

7.1. Advection equation

As explained in appendix B, the combination of advection schemes from *AeoLiS* and *CDM* has resulted in several problems. In order to solve these problems and decrease the uncertainties related to the advection scheme in *CDM* a new solver should be developed. This development requires research into several aspects:

- *CDM* assumed a steady state solution ($\delta c / \delta t = 0$), which increases computational speed significantly. The consequences of this assumption are unknown. It has to be researched if this assumption is valid and if it is justified to be implemented in the new solver.
- It is unknown what the consequences are of the differences in right-hand side in the advection schemes (net entrainment). The physical meaning of the right-hand side in *CDM* must be researched ($\frac{c}{T} \left(1 - \frac{c}{c_s}\right)$) and if the implementation of this formulation is required in the new solver.
- Because the grain speed is spatially varying, this grain speed should be included in the advection term ($u_s \frac{\delta c}{\delta t} \rightarrow \frac{\delta c u_s}{\delta t}$).

7.2. Sediment transport

The quantitative prediction capabilities of *AeoLiS* have been used in earlier research by computing the effect of sediment sorting, armouring and soil moisture on sediment transport at the Sand Motor (Hoonhout and de Vries, 2017). The formulation for the saturated concentration c_{sat} in the new model is an order of magnitude larger than the original formulation in *AeoLiS*, while the new grain speed u_s is an order of magnitude

smaller. In order to validate the predictive capabilities of the model, new sediment transport computations should be compared with the results from [Hoonhout and de Vries \(2017\)](#).

Besides, the multi-fraction sediment transport is not fully implemented in the model. The implementation of the multi-fraction sediment transport should be completed, by solving the entire advection scheme for multi fractions.

7.3. Vegetation, meteorology and groundwater

Meteorology influences sediment transport. Velocity threshold is affected as a result of precipitation and evaporation. Additionally, meteorological conditions such as snow, temperature and sun shine also influence growth of vegetation. Indirectly, precipitation influences the growth of vegetation by increasing the groundwater table. Once the groundwater table is known, an estimation can be made of the location of the salinity interface which also influences vegetation growth. The groundwater table also influences sediment transport, since it acts as a non-erodible layer. Capillary fringe increases the velocity threshold, which also reduces sediment transport.

The current vegetation module lacks vegetation competition and is only directly related to sediment burial. More research should be performed on the dependence of local vegetation growth on salinity concentrations, salt spray, human influences, meteorological effects and the groundwater table. Besides, the probabilistic approach on dispersion and germination of seeds and the lateral propagation is very simplistic. More research should be performed on the conditions governing these processes and the implementation should be improved.

The implementation of a more extensive vegetation module, meteorological effects and a groundwater table are interdependent and therefore a complete implementation of these processes combined is recommended.

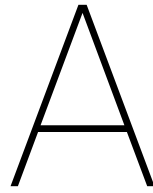
7.4. Flow separation

The current implementation of the flow separation is optimized for barchan dune simulations. Due to the lack of turbulence effects, the assumption that the shear velocity inside the separation bubble is possibly not true. The influence of turbulence inside and outside (wind gusts) the separation bubble should be investigated and implemented in the model. This can be done by simulating with smaller time steps or by implementing a turbulence factor on the flow velocity.

The shape and starting point of the separation bubble should be related to the wind velocity and topography. A better understanding and improved implementation of the separation of flow is important for a more realistic simulation of coastal areas.

7.5. Coupling with hydrodynamic models

The hydrodynamic processes implemented in the model are only suitable for situations with a steady shoreline under calm conditions. In order to improve the simulation of the interaction between aeolian and marine processes and to simulate the influence of seasonal variation of the shoreline and longer term variation, such as sea level rise induced by climate change, a coupling with a hydrodynamic model such as Delft3D ([Lesser et al., 2004](#)) is recommended. To simulate the influence of extreme events on dunes, a coupling with XBeach ([Roelvink et al., 2009](#)) is recommended.



Conceptual scheme of model

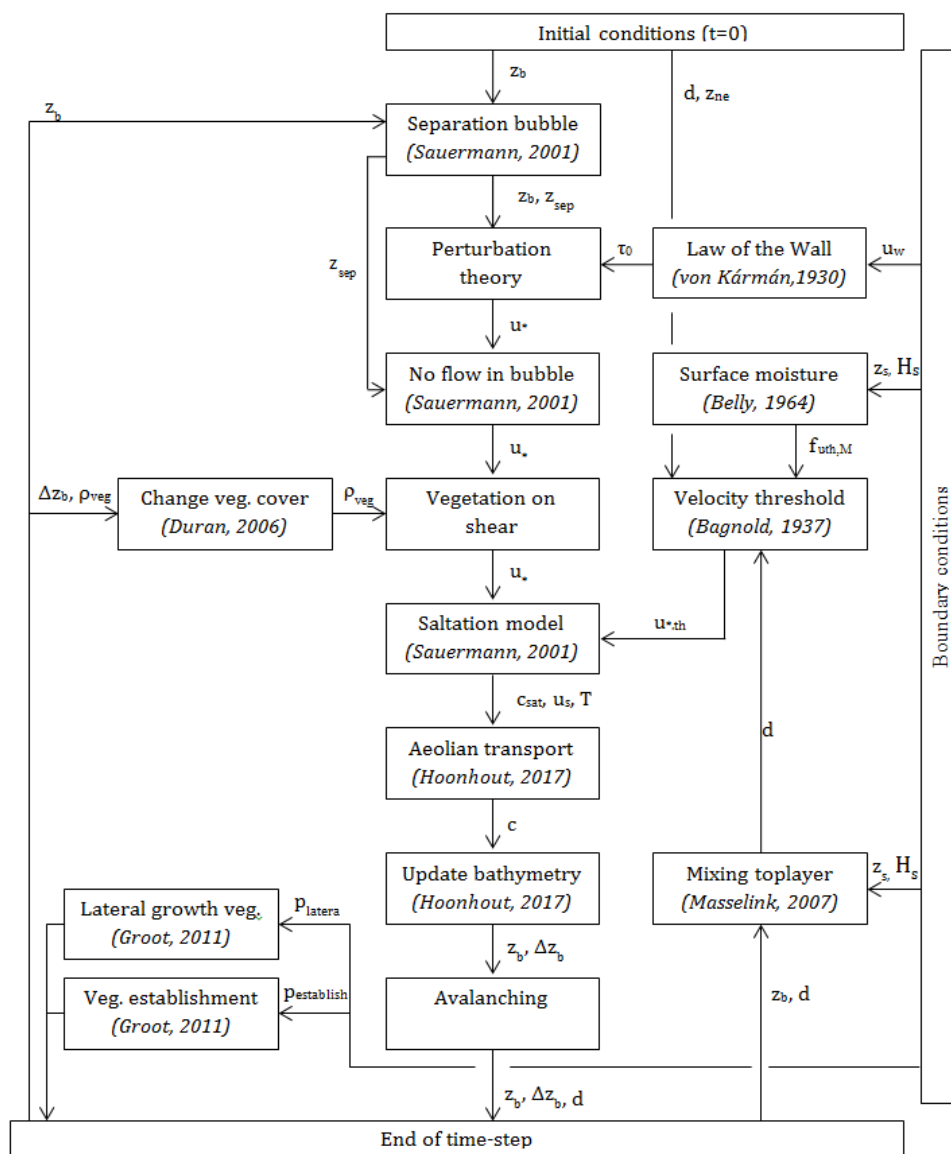


Figure A.1: Conceptual scheme of the model

B

Advection Scheme

The coupling of different aspects from the advection schemes of *AeoLiS* and *CDM* has led to some unsolved problems. In order to sketch a clear overview of these problems, first both approaches and their differences will be elaborated. Afterwards, the approach for the new model will be discussed, including the reasoning behind the decisions and the related consequences. At the end an overview of the resulting unsolved problems will be given.

B.1. Advection scheme comparison

AeoLiS

It is assumed by [de Vries et al. \(2014\)](#) that the sediment velocity and wind velocity are linear proportional and related the sediment concentration to the sediment transport rate via:

$$q = u_s C \quad (\text{B.1})$$

where q (kg/m/s) is the sediment transport rate, u_s (m/s) is the sediment velocity and C (kg/m²) is the sediment concentration. The grain speed u_s and the wind velocity at height z u_z (m/s) are assumed to have a linear relation:

$$u_s = u_z \zeta \quad (\text{B.2})$$

where ζ (-) is a constant. [de Vries et al. \(2014\)](#) proposed a linear advection model to compute the instantaneous sediment concentration c (kg/m²). [Hoonhout and de Vries \(2016b\)](#) adapted this scheme for *AeoLiS*, assuming $\zeta = 1$ (-), resulting in:

$$\frac{\delta c}{\delta t} + u_s \frac{\delta c}{\delta x} = E - D \quad (\text{B.3})$$

where t (s) is time, x (m) is the cross-shore distance and u_z (m/s) is the wind velocity at height z (m). E and D are the erosion and deposition terms, which combined represent the net entrainment.

The net entrainment is based on the difference between the saturated concentration c_{sat} and the actual concentration c , divided by a time adaptation scale T . It is maximized by the available sediment in the bed m_a :

$$E - D = \min\left(\frac{\delta m_a}{\delta t}; \frac{c_s - c}{T}\right) \quad (\text{B.4})$$

Neglecting the supply-limited situation:

$$\frac{\delta c}{\delta t} + u_s \frac{\delta c}{\delta x} = \frac{c_s - c}{T} \quad (\text{B.5})$$

where c_s is modified from [Bagnold \(1937\)](#):

$$c_s = \frac{C_b \sqrt{\frac{d}{D}} \frac{\rho_a}{g} (u_* - u_{*th})^3}{u_s} \quad (\text{B.6})$$

where C_b (-) is an empirical constant to account for the grain size distribution width, d (m) the grain size, D (m) a reference grain size and ρ_a (kg/m^3) the air density. u_* (m/s) and u_{*th} (m/s) are the shear velocity and shear velocity threshold ($u_* = \sqrt{\frac{\tau}{\rho_a}}$).

CDM

In order to simplify the comparison between AeoliS and CDM, the density of the grains in the saltation layer ρ (kg/m^3) is replaced by the concentration c (kg/m^3). [Sauermann et al. \(2001\)](#) proposed a closed model for the sand flux in the saltation layer:

$$\frac{\delta c}{\delta t} + \frac{\delta(cu_s)}{\delta x} = \frac{c}{T} \left(1 - \frac{c}{c_s}\right) \quad (\text{B.7})$$

where the saltation time T is defined as:

$$T = \frac{2\alpha u_s}{g} \frac{\tau}{\gamma(\tau - \tau_t)} \quad (\text{B.8})$$

where α represents an effective restitution coefficient and γ is a model parameter accounting for the splash process. The saturated concentration c_s is defined as:

$$c_s = \frac{2\alpha}{g} (\tau - \tau_t) \quad (\text{B.9})$$

For the sand velocity u_s , [Sauermann et al. \(2001\)](#) proposed the following model:

$$\frac{\delta u_s}{\delta t} + \left(u_s \frac{\delta}{\delta x}\right) u_s = \frac{3}{4} C_d \frac{\rho_a}{\rho_g} \frac{1}{d} (v_{eff} - u_s) |v_{eff} - u_s| - \frac{g}{2\alpha} \quad (\text{B.10})$$

where v_{eff} (m/s) is the effective wind velocity, obtained by:

$$v_{eff} = \frac{u_*}{\kappa} \sqrt{1 - \frac{\tau g_0}{\tau}} \left(2A_1 - 2 + \ln \frac{z_1}{z_0}\right) \quad (\text{B.11})$$

Several assumptions are made to make the model suitable for geomorphological applications. First, the stationary solution ($\frac{\delta}{\delta t}$) of [B.7](#) is used:

$$\frac{\delta(cu_s)}{\delta x} = \frac{c}{T} \left(1 - \frac{c}{c_s}\right) \quad (\text{B.12})$$

A distinction is made for the grain velocity inside and outside the separation bubble. Inside the separation bubble shear stress drops discontinuously to zero, which reduces [B.10](#) to:

$$\frac{1}{2} \frac{\delta u_s^2}{\delta x} = \frac{3}{4} C_d \frac{\rho_a}{\rho_g} \frac{1}{d} u_s^2 \quad (\text{B.13})$$

Outside the separation bubble, the convective term is neglected, which reduces [B.10](#) to:

$$u_s = v_{eff} - \sqrt{\frac{2gd\rho_g}{3\alpha C_d \rho_a}} \quad (\text{B.14})$$

B.2. Advection scheme in new model

The main objective of the new model is to create a model that is quantitatively capable of predicting dune development. For now, it is not entirely certain what the consequences are of the usage of a stationary solution. Therefore, the advection scheme in the new model is based on *AeoliS*, but the parameters within the advection scheme are based on formulations as used in *CDM*.

Steady state solution

CDM assumed a steady state solution ($\delta c / \delta t = 0$), which has a positive effect on computational speed. Since the consequences are not yet investigated, the new model does not adapt that assumption. For hourly averaged wind speed the assumptions seems reasonable, but first the exact consequences and expected errors must be assessed.

Spatially varying grain speed

With a spatially varying grain speed, equation B.5 changes to:

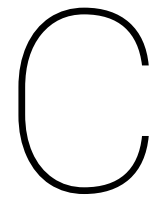
$$\frac{\delta c}{\delta t} + \frac{\delta c u_s}{\delta x} = \frac{\delta c}{\delta t} + u_s \frac{\delta c}{\delta x} + c \frac{\delta u_s}{\delta x} = \frac{c_s - c}{T} \quad (\text{B.15})$$

The third term ($c \frac{\delta u_s}{\delta x}$) is only negligible for small changes in shear velocity, which is not the case and especially not around the separation bubble.

In the model, this third term is neglected, but in the future this third term should be implemented and it is essential to investigate the consequences of this implementation.

Right-hand side (net entrainment)

The right hand sides in the advection schemes of *AeoLiS* and *CDM* are different, but it is not known what the consequences are of both approaches. Additionally, the parameter T has different names for both models (*AeoLiS*: time adaptation scale, *CDM*: saltation time) and it is not known if T in *CDM* and *AeoLiS* represent the same conceptual parameter.



Redefined Grid Parameters

In order to simulate all relevant processes in the coastal zone, coupling of AeoliS with other models is desired. Models like XBeach and Delft3D are compatible with curvilinear grids and therefore the grid parameters within AeoliS need to be redefined to make future coupling possible. The new defined grid in AeoliS is modified from XBeach.

However, the rotation of the computational grid for the analytical flow perturbation model requires an equidistant grid, in order to increase computational speed. Therefore within the current implementation, despite the redefined grid parameters, the model is not compatible with a curvilinear grid.

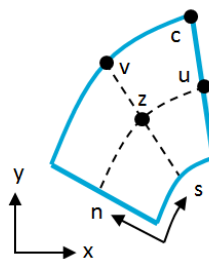


Figure C.1: Names of the characteristic points in a computational cell.

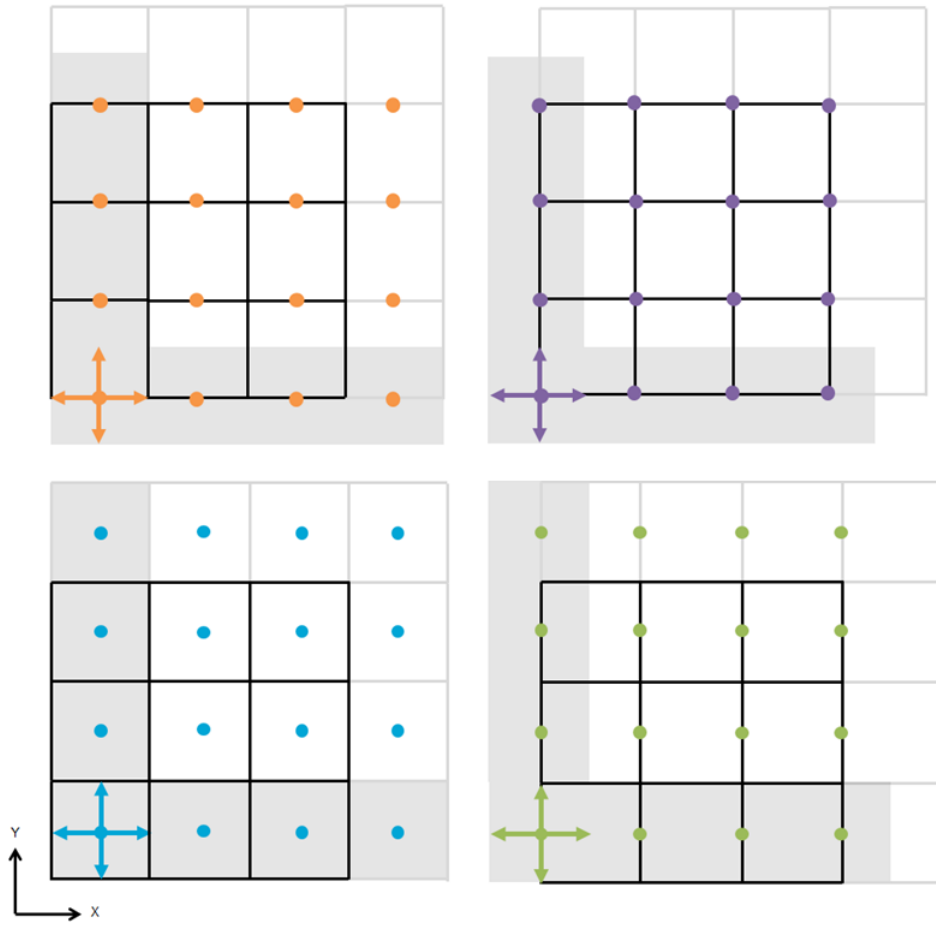


Figure C.2: Distances in the computational grid.

	●	●	●	●
●	z	u	v	c
↔	dsz	dsu	dsv	dsc
↕	dnz	dnu	dnv	dnc
■	dsdnz	dsdnu	dsdnv	dsdnc

Figure C.3: Abbreviations of the points and distances in the computational grid.

Bibliography

- Arens, S. and Mannaart, M. (2008). De zeereep van Groote Keeten Vormen en processen. *Stichting Duinbehoud en Arens, bureau voor strand- en duinonderzoek*.
- Arens, S. M. (2017). De zeereep van Groote Keeten. (March).
- Baas, A. C. (2002). Chaos, fractals and self-organization in coastal geomorphology: Simulating dune landscapes in vegetated environments. *Geomorphology*, 48(1-3):309–328.
- Bagnold, R. a. (1936). The Movement of Desert Sand. *Proceedings of the Royal Society A: Mathematical, Physical and Engineering Sciences*, 157(892):594–620.
- Bagnold, R. A. (1937). The Transport of Sand by Wind. *The Geographical Journal*, 89(5):409.
- Bakker, T. W., Klijn, J. A., and Van Zadelhoff, F. J. (1981). *Nederlandse kustduinen-Landschapsecologie*. Centrum voor Landbouwpubl. en Landbouwdocumentatie.
- Baldwin, K. A. and Maun, M. A. (1983). Microenvironment of Lake Huron sand dunes. *Canadian Journal of Botany*, 61(1):241–255.
- Bauer, B. O. and Davidson-Arnott, R. G. D. (2003). A general framework for modeling sediment supply to coastal dunes including wind angle, beach geometry, and fetch effects. *Geomorphology*, 49(1):89–108.
- de Groot, A., Berendse, F., Riksen, M., Baas, A., Slim, P., Dobben, H. V., and Stroosnijder, L. (2011). Modelling coastal dune formation and associated vegetation development. *Geophysical Research Abstracts*, 13(6):4959.
- de Groot, A., de Vries, S., Keijsers, J., Riksen, M., van Ye, Q., Poortinga, A., Arens, S., Bochev-Van der Burgh, L., Wijnberg, K., Schretlen, J., and van Thiel de Vries, J. (2012). Measuring and modeling coastal dune development in the Netherlands. *NCK-days 2012 : Crossing borders in coastal research : jubilee conference proceedings*, page 6.
- de Vries, S., van Thiel de Vries, J. S. M., van Rijn, L. C., Arens, S. M., and Ranasinghe, R. (2014). Aeolian sediment transport in supply limited situations. *Aeolian Research*, 12:75–85.
- Durán, O. (2008). Parabolic dunes in north-eastern Brazil. *Geomorphology*, 102:460—471.
- Durán, O. and Herrmann, H. (2006a). Modelling of saturated sand flux. *Journal of Statistical Mechanics: Theory and Experiment*, (7).
- Durán, O. and Herrmann, H. J. (2006b). Vegetation against dune mobility. *Physical Review Letters*, 97(18):1–4.
- Durán, O. and Moore, L. J. (2013). Vegetation controls on the maximum size of coastal dunes. *Proceedings of the National Academy of Sciences*, 110(43):17217–17222.
- Durán, O., Parteli, E. J., and Herrmann, H. J. (2010). A continuous model for sand dunes: Review, new developments and application to barchan dunes and barchan dune fields. *Earth Surface Processes and Landforms*, 35(13):1591–1600.
- Durán, O., Schwämmle, V., Lind, P. G., and Herrmann, H. J. (2011). Size distribution and structure of Barchan dune fields. *Nonlinear Processes in Geophysics*, 18(4):455–467.
- Ecoshape. Building with Nature. <https://www.ecoshape.org/en/>.
- Goldstein, E. B. and Moore, L. J. (2016). Stability and bistability in a one-dimensional model of coastal fore-dune height. *Journal of Geophysical Research: Earth Surface*, 121(5):964–977.

- Goldstein, E. B., Moore, L. J., and Vinent, O. D. (2017). Lateral vegetation growth rates exert control on coastal foredune hummockiness and coalescing time. *Earth Surface Dynamics*, 5(3):417–427.
- Google Earth. Satellite image. <https://www.google.com/earth/>.
- Hardisty, J. (1994). Beach and nearshore sediment transport. *Sediment transport and depositional processes*. Blackwell, London, UK, pages 216–255.
- Hersen, P. (2004). On the crescentic shape of barchan dunes. *European Physical Journal B*, 37(4):507–514.
- Hersen, P. (2005). Flow effects on the morphology and dynamics of aeolian and subaqueous barchan dunes. *Journal of Geophysical Research: Earth Surface*, 110(4):1–10.
- Hoonhout, B. and de Vries, S. (2017). Aeolian sediment supply at a mega nourishment. *Coastal Engineering*, 123(December 2016):11–20.
- Hoonhout, B. M. Model description AeoliS. <https://aeolis.readthedocs.io/en/latest/>.
- Hoonhout, B. M. (2017). Aeolian Sediment Availability and Transport. Technical report.
- Hoonhout, B. M. and de Vries, S. (2016a). A process-based model for aeolian sediment transport and spatiotemporal varying sediment availability. *Journal of Geophysical Research: Earth Surface*, 121(8):1555–1575.
- Hoonhout, B. M. and de Vries, S. (2016b). A process-based model for aeolian sediment transport and spatiotemporal varying sediment availability. *Journal of Geophysical Research: Earth Surface*, 121(8):1555–1575.
- Hoonhout, B. and Waagmeester, N. (2014). Invloed van strandbebouwing op zandverstuiving.
- Keijsers, J. G. S. (2015). *Modelling foredune dynamics in response to climate change*.
- Keijsers, J. G. S., De Groot, A. V., and Riksen, M. (2015). Vegetation and sedimentation on coastal foredunes. *Geomorphology*, 228:723–734.
- Keijsers, J. G. S., Groot, A. V. D., and Riksen, M. J. P. M. (2016). Journal of Geophysical Research : Earth Surface Modeling the biogeomorphic evolution of coastal dunes. pages 1–21.
- Kroy, K., Sauermann, G., and Herrmann, H. J. (2002). Minimal model for aeolian sand dunes.
- Lesser, G. R., Roelvink, J. v., Van Kester, J., and Stelling, G. (2004). Development and validation of a three-dimensional morphological model. *Coastal engineering*, 51(8-9):883–915.
- Loffler, M. A. M., Goessen, P., Hoogstrate, T., and van der Valk, B. (2016). Dynamisch kustbeheer - Kustveiligheid en natuur profiteren van stuivend zand. *Water Matters*, 2(December 2016):1–5.
- Luna, M. C. M., Parteli, E. J., and Herrmann, H. J. (2012). Model for a dune field with an exposed water table. *Geomorphology*, 159-160:169–177.
- Marco, M. C., Parteli, E. J., Durán, O., and Herrmann, H. J. (2011). Model for the genesis of coastal dune fields with vegetation. *Geomorphology*, 129(3-4):215–224.
- Maun, M. A. (2009). *The biology of coastal sand dunes*. Oxford University Press.
- Ministerie van Economische Zaken and Ministerie van Infrastructuur en Milieu (2017). Programma Aanpak Stikstof. (december).
- Moore, L. J., Durán Vinent, O., and Ruggiero, P. (2016). Vegetation control allows autocyclic formation of multiple dunes on prograding coasts. *Geology*, 44(7):559–562.
- Nield, J. M. and Baas, A. C. W. (2008). Investigating parabolic and nebkha dune formation using a cellular automaton modelling approach. *Earth Surface Processes and Landforms*, 33(5):724–740.

- Nolet, C., van Puijenbroek, M., Suomalainen, J., Limpens, J., and Riksen, M. (2017). UAV-imaging to model growth response of marram grass to sand burial: Implications for coastal dune development. *Aeolian Research*, (June):1–12.
- Parsons, A. J. and Abrahams, A. D. (2009). *Geomorphology of desert environments*.
- Parteli, E. J., Durán, O., Bourke, M. C., Tsoar, H., Pöschel, T., and Herrmann, H. (2014a). Origins of barchan dune asymmetry: Insights from numerical simulations. *Aeolian Research*, 12:121–133.
- Parteli, E. J. and Herrmann, H. J. (2007). Dune formation on the present Mars. *Physical Review E - Statistical, Nonlinear, and Soft Matter Physics*, 76(4):1–16.
- Parteli, E. J., Kroy, K., Tsoar, H., Andrade, J. S., and Pöschel, T. (2014b). Morphodynamic modeling of aeolian dunes: Review and future plans. *European Physical Journal: Special Topics*, 223(11):2269–2283.
- Parteli, E. J. R., Duran, O., and Herrmann, H. J. (2007). Minimal size of a barchan dune. pages 1–11.
- Parteli, E. J. R., Duran, O., Tsoar, H., Schwämmle, V., and Herrmann, H. J. (2009). Dune formation under bimodal winds. *Proceedings of the National Academy of Sciences*, 106(52):22085–22089.
- PWN (2018). PWN. <https://www.pwn.nl/over-pwn/pers-en-nieuws/natuur-recreatie/veilige-en-vitale-duinen-door-de-aanleg-van-stuifkuilen?nid=1370>.
- Ranasinghe, R., Callaghan, D., and Stive, M. J. F. (2012). Estimating coastal recession due to sea level rise: Beyond the Bruun rule. *Climatic Change*, 110(3-4):561–574.
- Raupach, M. R., Gillette, D. A., and Leys, J. F. (1993). The effect of roughness elements on wind erosion threshold. *Journal of Geophysical Research*, 98(D2):3023–3029.
- Rijkswaterstaat (1990). A new coastal defence policy for the Netherlands. *Dutch Ministry of Transport and Public Works Policy Report*.
- Rijkswaterstaat and STOWA. Randvoorwaarden Dynamisch Kustbeheer. <https://www.dynamischkustbeheer.nl/>.
- Roelvink, D., Reniers, A., Van Dongeren, A., de Vries, J. v. T., McCall, R., and Lescinski, J. (2009). Modelling storm impacts on beaches, dunes and barrier islands. *Coastal engineering*, 56(11-12):1133–1152.
- Sauermann, G., Andrade, J. S., Maia, L. P., Costa, U. M., Araújo, A. D., and Herrmann, H. J. (2003). Wind velocity and sand transport on a barchan dune. *Geomorphology*, 54(3-4):245–255.
- Sauermann, G., Kroy, K., and Herrmann, H. J. (2001). Continuum saltation model for sand dunes. *Physical Review E - Statistical Physics, Plasmas, Fluids, and Related Interdisciplinary Topics*, 64(3):10.
- Sauermann, G., Rognon, P., Poliakov, A., and Herrmann, H. J. (2000). The shape of the barchan dunes of Southern Morocco. *Geomorphology*, 36(1-2):47–62.
- Schwämmle, V. and Herrmann, H. J. (2005). A model of barchan dunes including lateral shear stress. *European Physical Journal E*, 16(1):57–65.
- Sherman, D. J. and Li, B. (2012). Predicting aeolian sand transport rates: A reevaluation of models. *Aeolian Research*, 3(4):371–378.
- Staatsbosbeheer. Schoorlse Duinen. <https://schoorlsteduinen.staatsbosbeheer.nl/default.aspx>.
- Stive, M. J., de Schipper, M. A., Luijendijk, A. P., Aarninkhof, S. G., van Gelder-Maas, C., van Thiel de Vries, J. S., de Vries, S., Henriquez, M., Marx, S., and Ranasinghe, R. (2013). A New Alternative to Saving Our Beaches from Sea-Level Rise: The Sand Engine. *Journal of Coastal Research*, 290:1001–1008.
- van den Hurk, B., Tank, A. K., Lenderink, G., van Ulden, A., van Oldenborgh, G. J., Katsman, C., van den Brink, H., Keller, F., Bessembinder, J., Burgers, G., Komen, G., Hazeleger, W., and Drijfhout, S. (2007). New climate change scenarios for the Netherlands. *Water Science and Technology*, 56(4):27–33.

- van Oene, H., Berendse, F., and de Kovel, C. G. F. (1999). Model Analysis of the Effects of Historic CO₂ Levels and Nitrogen Inputs on Vegetation Succession. *Ecological Applications*, 9(3):920.
- van Puijenbroek, M. E. (2017). *Dunes, above and beyond*.
- van Puijenbroek, M. E., Limpens, J., de Groot, A. V., Riksen, M. J., Gleichman, M., Slim, P. A., van Dobben, H. F., and Berendse, F. (2017a). Embryo dune development drivers: beach morphology, growing season precipitation, and storms. *Earth Surface Processes and Landforms*, 42(11):1733–1744.
- van Puijenbroek, M. E., Nolet, C., De Groot, A. V., Suomalainen, J. M., Riksen, M. J., Berendse, F., and Limpens, J. (2017b). Exploring the contributions of vegetation and dune size to early dune development using unmanned aerial vehicle (UAV) imaging. *Biogeosciences*, 14(23):5533–5549.
- van Puijenbroek, M. E., Teichmann, C., Meijdam, N., Oliveras, I., Berendse, F., and Limpens, J. (2017c). Does salt stress constrain spatial distribution of dune building grasses *Ammophila arenaria* and *Elytrichia juncea* on the beach? *Ecology and Evolution*, 7(18):7290–7303.
- van Slobbe, E., de Vriend, H. J., Aarninkhof, S., Lulofs, K., de Vries, M., and Dircke, P. (2013). Building with Nature: In search of resilient storm surge protection strategies. *Natural Hazards*, 65(1):947–966.
- Weng, W. S., Hunt, J. C. R., Carruthers, D. J., Warren, A., Wiggs, G. F. S., Livingstone, I., and Castro, I. (1991). Air flow and sand transport over sand-dunes. In Barndorff-Nielsen, O. E. and Willetts, B. B., editors, *Aeolian Grain Transport*, pages 1–22, Vienna. Springer Vienna.